

Institutionen för systemteknik

Department of Electrical Engineering

Examensarbete

Powertrain modeling for realtime simulation

Examensarbete utfört i Fordonssystem
vid Tekniska högskolan vid Linköpings universitet
av

Simon Lind

LiTH-ISY-EX-14/4808-SE

Linköping 2014



Linköpings universitet
TEKNISKA HÖGSKOLAN

Powertrain modeling for realtime simulation

Examensarbete utfört i Fordonssystem
vid Tekniska högskolan vid Linköpings universitet
av

Simon Lind

LiTH-ISY-EX-14/4808-SE

Handledare: **Andreas Myklebust**
ISY, Linköpings universitet
Anders Andersson
VTI, Statens väg- & transportforskningsinstitut
Sogol Kharrazi
VTI, Statens väg- & transportforskningsinstitut

Examinator: **Per Öberg**
ISY, Linköpings universitet

Linköping, 24 oktober 2014

| | | |
|---|--|----------------------|
|  | Avdelning, Institution Division, Department | Datum Date |
| | Division of Vehicular Systems Department of Electrical Engineering SE-581 83 Linköping | 2014-10-24 |

| | | |
|--|---|---|
| Språk Language <input type="checkbox"/> Svenska/Swedish <input checked="" type="checkbox"/> Engelska/English <input type="checkbox"/> _____ | Rapporttyp Report category <input type="checkbox"/> Licentiatavhandling <input checked="" type="checkbox"/> Examensarbete <input type="checkbox"/> C-uppsats <input type="checkbox"/> D-uppsats <input type="checkbox"/> Övrig rapport <input type="checkbox"/> _____ | ISBN _____ ISRN LiTH-ISY-EX-14/4808-SE Serietitel och serienummer ISSN Title of series, numbering _____ |
|--|---|---|

URL för elektronisk version

<http://www.vehicular.isy.liu.se>

| | |
|-----------------------------|---|
| Titel Title | Modellering av drivlinemodell för realtidssimulering Powertrain modeling for realtime simulation |
| Författare Author | Simon Lind |

Sammanfattning
 Abstract

The goal of this thesis was to develop a powertrain model of a vehicle and parametrize it using non-invasive sensors. The non-invasive sensors available were chassis dynamometer, the pedal robot and the vehicle's on-board diagnostics which was accessed using a scan tool. Non-invasive sensors were used so that the vehicle to model can easily be changed. A parametrization methodology to parametrize the model for a new vehicle was also developed to facilitate the change of vehicle. The powertrain model is for cars with a combustion engine and a manual gearbox.

The engine model consist of two static maps, a pedal map and an engine map. The pedal map is created using the fact that a constant pedal position and engine speed gives a constant throttle position. The engine map is created in similar manner using that a constant throttle position and engine speed gives a constant engine torque. The engine model also uses a first order lag element to model the time delay from a change in pedal position to a change in wheel torque. The driveline model is a rigid driveline model that assumes that the clutch, driveshaft and propeller shaft are stiff.

The developed parametrization methodology contains information on how to estimate the parameters of the model which are gear ratios, engine and driveline inertias, engine and driveline losses, engine and pedal maps and the time constant for the time delay.

The powertrain model was validated component wise, as standalone and integrated into the vehicle model against data gathered with the help of the chassis dynamometer. For the standalone and integrated validation the gathered data were for different driving cases, such as up and down gear-shifting, engine braking and skipping gears. The standalone validation showed that the model performed well for the presented driving cases and the results had good data fit for 3rd gear and higher. However not for 1st and 2nd gear due to problems in the pedal map. The pedal map was constructed on the assumption that the same pedal position for all gears gives the same throttle position, which was not always the case. This caused problems in some areas of the engine and pedal maps however in the validation of the maps it was shown that the maps for the most part gave good results.

| | |
|------------------------------|--|
| Nyckelord Keywords | Engine model, driveline model, realtime simulation |
|------------------------------|--|

Abstract

The goal of this thesis was to develop a powertrain model of a vehicle and parametrize it using non-invasive sensors. The non-invasive sensors available were chassis dynamometer, the pedal robot and the vehicle's on-board diagnostics which was accessed using a scan tool. Non-invasive sensors were used so that the vehicle to model can easily be changed. A parametrization methodology to parametrize the model for a new vehicle was also developed to facilitate the change of vehicle. The powertrain model is for cars with a combustion engine and a manual gearbox.

The engine model consist of two static maps, a pedal map and an engine map. The pedal map is created using the fact that a constant pedal position and engine speed gives a constant throttle position. The engine map is created in similar manner using that a constant throttle position and engine speed gives a constant engine torque. The engine model also uses a first order lag element to model the time delay from a change in pedal position to a change in wheel torque. The driveline model is a rigid driveline model that assumes that the clutch, driveshaft and propeller shaft are stiff.

The developed parametrization methodology contains information on how to estimate the parameters of the model which are gear ratios, engine and driveline inertias, engine and driveline losses, engine and pedal maps and the time constant for the time delay.

The powertrain model was validated component wise, as standalone and integrated into the vehicle model against data gathered with the help of the chassis dynamometer. For the standalone and integrated validation the gathered data were for different driving cases, such as up and down gear-shifting, engine braking and skipping gears. The standalone validation showed that the model performed well for the presented driving cases and the results had good data fit for 3rd gear and higher. However not for 1st and 2nd gear due to problems in the pedal map. The pedal map was constructed on the assumption that the same pedal position for all gears gives the same throttle position, which was not always the case. This caused problems in some areas of the engine and pedal maps however in the validation of the maps it was shown that the maps for the most part gave good results.

Acknowledgments

First and foremost I would like to thank my supervisors, Anders Andersson and Sogol Kharrazi at VTI and Andreas Myklebust at LiU, for support and assistance throughout this thesis. I would also like to thank my examiner Per Öberg for assistance in the chassis dynamometer laboratory. Finally i would like to thank David Mattsson at the Division of Vehicular Systems at LiU for helping me carry out measurements in the chassis dynamometer.

Linköping, October 2014
Simon Lind

Contents

| | |
|--|-----------|
| Notation | ix |
| 1 Introduction | 1 |
| 1.1 Background | 1 |
| 1.2 Purpose and goal | 2 |
| 1.3 Related research | 2 |
| 1.3.1 Engine models | 3 |
| 1.3.2 Driveline models | 4 |
| 1.4 Outline | 5 |
| 2 System overview | 7 |
| 2.1 Driving simulator | 7 |
| 2.2 Chassis dynamometer laboratory | 10 |
| 2.3 Pedal robot | 13 |
| 2.4 On-board diagnostics | 13 |
| 2.5 Golf V | 14 |
| 3 Powertrain model | 17 |
| 3.1 Driveline model | 17 |
| 3.2 Engine model | 18 |
| 3.3 Engine loss model | 23 |
| 4 Parametrization methodology | 25 |
| 4.1 Combined gear and final drive ratios | 25 |
| 4.2 Driveline and engine inertia | 27 |
| 4.2.1 Alternative method: Engine inertia | 36 |
| 4.3 Driveline and engine losses | 38 |
| 4.4 Engine and Pedal maps | 41 |
| 4.5 Engine lag element | 45 |
| 5 Model validation | 47 |
| 5.1 Engine and pedal map validation | 47 |
| 5.2 Standalone powertrain model validation | 58 |

| | | |
|----------|--|-----------|
| 5.3 | Integrated powertrain model validation | 62 |
| 6 | Conclusion | 67 |
| 6.1 | Future Work | 68 |
| | Bibliography | 71 |

Notation

| Variable | Description |
|----------------------------|---|
| A_f | Frontal area of the vehicle |
| B | Engine bore |
| $BMEP$ | Brake mean effective pressure |
| c_d | Air drag coefficient |
| c_r | Rolling resistance coefficient |
| F_{air} | Aerodynamic drag force |
| F_{grav} | Gravitational resistance |
| F_{prop} | Propulsion force |
| F_{res} | Driving resistance |
| F_{roll} | Rolling resistance |
| g | Gravitational constant |
| i_t | Transmission conversion ratio |
| i_f | Final drive conversion ratio |
| J_d | Driveline inertia |
| J_e | Engine inertia |
| J_{pwr} | Powertrain inertia |
| J_w | Wheel inertia |
| m | Vehicle mass |
| $M_{acc,drv}$ | Wheel torque required to accelerate the driveline |
| $M_{acc,pwr}$ | Wheel torque required to accelerate the powertrain |
| M_c | Clutch torque |
| M_e | Engine torque |
| $M_{fric}(\dot{\theta}_w)$ | Steady state friction torque for wheel speed $\dot{\theta}_w$ |
| $M_{loss:drv}$ | Driveline losses |
| M_w | Wheel torque |
| $M_{w,Dyn}$ | Wheel torque from a dynamic measurement |
| $M_{w,i}$ | Torque at wheel i |
| n_r | Number of revolutions per cycle |
| p_{em} | Exhaust manifold pressure |
| p_{im} | Intake manifold pressure |
| r_w | Wheel radius |

| Variable | Description |
|------------------------|--|
| S | Engine piston stroke |
| S_p | Mean piston speed |
| v_0 | Wind speed relative to the ground during experiment |
| V_D | Engine displacement |
| $W_{i,g}$ | Gross indicated work |
| $W_{i,p}$ | Pumping work |
| W_{fr} | Friction work |
| δ_{cl} | Clutch signal |
| θ_e | Angle of the engine |
| $\dot{\theta}_e$ | Angular velocity of the engine |
| $\dot{\theta}_{e,int}$ | Angular velocity of the engine calculated from the engine torque |
| $\dot{\theta}_{e,wh}$ | Angular velocity of the engine calculated from the wheel speed |
| $\ddot{\theta}_e$ | Angular acceleration of the engine |
| θ_w | Angle of the wheel |
| $\dot{\theta}_w$ | Angular velocity of the wheel |
| $\ddot{\theta}_w$ | Angular acceleration of the wheel |
| ξ_{aux} | Load from auxiliary devices |
| Π_{bl} | Boost layout |
| ρ_a | Density of air |
| τ_c | Time constant |

| Abbreviation | Description |
|--------------|---------------------------------|
| DTC | Diagnostics trouble code |
| ECU | Engine control unit |
| OBD | On-board diagnostics |
| PID | Parameter identification number |
| RMSE | Root mean square error |
| RPM | Revolutions per minute |

1

Introduction

This chapter gives an introduction to this thesis and contains background information, thesis outline, related work and the objective of this thesis.

1.1 Background

The longitudinal propulsion of a vehicle is generated by its powertrain. The powertrain consists of the components in a vehicle that generate power and deliver it to the road. The powertrain typically consists of engine, transmission, drive shafts, differential and wheels. The components of the powertrain when the engine has been excluded is called the driveline or drivetrain. There are many powertrain configurations with different components, choice of driven wheels, fuel sources and engine mounting positions. Each with their own advantages and disadvantages. Currently electrical vehicles and hybrid electrical vehicles are of interest as environmental concerns such as air pollution in urban areas and global warming are major problems. By using electrical vehicles and hybrid electrical vehicles the emissions of green house gases and smog build up in major urban areas may be reduced because they have lower environmental footprints than conventional vehicles. In [22] the effect of plug-in hybrid electrical vehicles on a cities power grid is shown to decrease the net generated NO_x emissions during the ozone season. The powertrain configurations of electrical and hybrid electrical vehicles can be designed with different energy sources such as fuel cells, batteries, ultracapacitors, flywheels and engine-generators as shown in [9]. With a large selection of powertrain configurations being available and with new powertrain configurations being developed the ability to test them in simulations is useful when investigating their performance.

The Swedish National Road and Transport Research Institute (VTI) in collaboration with Linköpings University (LiU) have developed a platform for co-simulation [1]. The platform consists of a driving simulator located at VTI's office in Linköping and a chassis dynamometer at LiU. The driving simulator and the chassis dynamometer are connected with each other with the help of a pedal robot mounted in the vehicle in the chassis dynamometer. The pedal robot controls the pedal position in the vehicle from the inputs from the driver in the simulator. The co-simulator platform gives the ability to test powertrain configurations by mounting a vehicle in the chassis dynamometer.

If the driving simulator is not used in co-simulation with the chassis dynamometer it needs a parametrized model of a vehicle. To keep the process of parametrizing a model for a vehicle quick and simple no extra sensors are to be installed in the vehicle. This limits the sensors to non-invasive sensors such as the chassis dynamometer and pedal robot. In addition most vehicles today use on-board diagnostics systems that provide diagnostics data and diagnostics trouble codes. The diagnostics data can be used to parametrize the model however the amount of information available in a vehicle varies between manufacturers. In this thesis a powertrain model and a parametrization methodology for the model is developed.

1.2 Purpose and goal

The goal of this thesis is to derive a model of the powertrain in a vehicle and parametrize it. The data used in the parametrization is from non-invasive sensors such as chassis dynamometer, the pedal robot and the vehicle's on-board diagnostics. Non-invasive sensors are used so that the vehicle to model can easily be changed. A parametrization methodology to parametrize the model for a new vehicle is developed to facilitate the change of vehicle. To be able to use the model in VTI's driving simulator the model has to be applicable in real time. The powertrain model is for cars with a combustion engine and a manual gearbox.

1.3 Related research

Engine and driveline models are used in various applications such as driveline control, [18], engine control, [23], or investigation of various driveline properties [20], [10]. Relevant engine and driveline models to this thesis are models that can be used in real-time and with the limited data available, which limits the model complexity. In section 1.3.1 and 1.3.2 some engine and driveline models are presented.

1.3.1 Engine models

In [21] a scalable model of a generic internal combustion engine is developed. The engine torque of the model depends on the engine speed and the fuel mass per injection according to a quadratic Willan's model. The model is scalable because the engine displacement volume and the engine stroke can be viewed as size parameters.

The model developed in [21] has been modified and used in [16] and [17] to handle a turbocharged engine. This is done by adding an additional torque loss to the model with a first order delay to simulate the pressure dynamics in the turbocharger. The model used in [16] and [17] is a simple and generic model that has a fast simulation time due to easy calculations.

In [6] an analytic model for the cylinder pressure in a spark ignited engine is developed. The model uses the fact that the compression and expansion part of the ideal Otto cycle can be modeled with good accuracy by a polytropic process. A polytropic process is a thermodynamic process that follows the relation $pV^n = \text{Constant}$, where p is the pressure, V is the volume and n is the polytropic index. The combustion part of the ideal Otto cycle can be produced by interpolation between the compression and expansion part. The resulting model will be a function of crank angle, manifold pressure, manifold temperature and spark timing.

The cylinder pressure model developed in [6] has been used as the engine model in [10] and [15] with good results. In [15] the model was used for real time simulation of cylinder misfire, which demonstrate its on-line usability.

In [23] a dynamic model for a turbocharged diesel engine was developed. The model uses the steady state characteristics, estimated from performance maps, of the engine at the beginning and end of a change in input or load demand [23]. The performance maps are complemented with equations for engine dynamics, air systems and a time delay for the torque. The engine model can be expressed as a transfer function with the fuel command as the input and the engine speed as the output.

In this thesis the concept of using performance maps in the engine model from [23] was used to develop an engine model. A map based engine model was developed because the described engine models in this section require data that are not available. The engine model from [23] was chosen as a starting point because the other engine models could not easily be adapted to work with the available data. For example the scalable model in [21] need the injected fuel mass to calculate the engine torque which is not available from the data. Another example is the analytic model for the cylinder pressure in [6] that needs the crank shaft angle among other. The engine model in [23] is however for a turbocharged diesel engine and the vehicle to model has a non-turbocharged petrol engine. The difference is that the diesel engine do not need to wait on the intake manifold pressure to build up as it either lacks a throttle or it has different control goals for the throttle than a petrol engine.

1.3.2 Driveline models

In [7] a rigid driveline model called Basic Driveline Model is presented. In the rigid driveline model the clutch, driveshaft and propeller shaft are assumed to be stiff. In addition the gear and final drive ratio are assumed to multiply the torque without losses [7].

In [20] a longitudinal driveline models with different complexities that explain driveline oscillations is developed. The models consists of combinations of rotating inertias connected by damped shaft flexibilities.

The model called Drive-shaft model in [20] is the simplest model that consists of a lumped engine and transmission inertia and a wheel inertia. The inertias are connected by a damped torsional flexibility. The model uses the drive shaft torsion, the engine speed and the wheel speeds as states.

A more complex model in [20] is the Nonlinear clutch and Drive-shaft model. The model is derived from the Drive-shaft model by replacing the lumped engine and transmission inertia with an engine inertia connected to a lumped transmission, propeller shaft and final drive inertia. The inertias are connected by a nonlinear clutch flexibility. The model uses the clutch torsion, drive shaft torsion, the engine speed, transmission speed and the wheel speeds as states.

The above mentioned models from [20] describes the driveline in increasing detail. In [20] it is suggested that the Drive-shaft model is suitable for control design and that the Nonlinear clutch and Drive-shaft model is suitable for simulation studies in control design [20]. In [13] a driveline model from [20] is extended and used for analysis of the interaction between road slope data and vehicle shuffle. In [14] the extended driveline model used for the analysis is combined with a developed dry clutch model with thermal dynamics presented in [12]. The models are combined to study the effect of thermal expansion in the clutch on launch control.

In [3] commonly used friction clutch models are described and tested to see if they can be used in real time simulation. A torsional model of the powertrain with 3 degrees of freedom is used for the clutch model tests. The powertrain model used in [3] is described in [5], where it is used for examination of optimal control of the engagement of a dry clutch.

In [4] a torsional powertrain model with 4 degrees of freedom is used to examine clutch judder. The model uses 4 rotating inertias connected by shaft elements or frictional contact.

In [11] some of the most commonly used backlash models is described. The most widespread way to model backlash is to model it as a dead-zone. The simplest model described in [11] is a backlash connected to a flexible shaft that is considered to be a torsional spring. However for a more physical model of the backlash that also is valid for shafts with dampening a physical backlash model is presented. The physical backlash model includes an additional state variable that describes the position in the backlash. The physical backlash model was used in a simple powertrain model that consisted of two rotating inertias connected by a shaft with backlash.

The simple powertrain model with physical backlash presented in [11], is used in [18] for model based driveline control. It was concluded that it captured the essential properties of the system despite its low complexity.

This thesis uses the driveline model described in [7]. The driveline model was chosen because according to [7] many studies in propulsion show that it is sufficient to neglect the internal states of a driveline and treat it as a rigid driveline. The driveline model from [7] also has very low computational complexity which makes it applicable in real-time.

1.4 Outline

This thesis includes the following chapters:

Chapter 1 - Introduction: An introduction to this thesis containing background information, thesis outline, related work and the objective of this thesis.

Chapter 2 - System overview: Presents information about the VTI Driving simulator, the LiU chassis dynamometer laboratory, the pedal robot and the vehicle.

Chapter 3 - Powertrain model: Presents the engine and driveline models used in this thesis and explains the theory behind them.

Chapter 4 - Parametrization methodology: Presents a methodology to parametrize the model for a car.

Chapter 5 - Model validation: Presents validation data for the maps, powertrain model and vehicle model.

Chapter 6 - Conclusion: Presents the conclusion of this thesis.

2

System overview

This chapter describes the VTI driving simulator, the LiU chassis dynamometer laboratory, the pedal robot and the vehicle.

2.1 Driving simulator

The powertrain model was tested in VTI's driving simulator, Simulator III, located at VTI's office in Linköping. Simulator III is a 4 degrees of freedom moving base simulator, including linear and angular motions. The driver is situated in a Saab 9-3 cabin with a 120 degree field of view provided by six projectors. Three LCD displays serves as rear-view mirrors. A vibration table provides high-frequency vibration if needed. Vehicle and environment sound is provided by the vehicle speaker and a few complementing speakers to give a surround sound setup. Pictures of Simulator III can be seen in Figures 2.1 and 2.2.

One of the vehicle model used in the driving simulator is implemented as a Simulink model which can be seen in Figure 2.3. This thesis will use the vehicle model as base and replace the powertrain model in the Driveline block with the developed powertrain model.



Figure 2.1: Outside view of the driving simulator Simulator III at VTI.



Figure 2.2: Inside view of the driving simulator Simulator III at VTI.

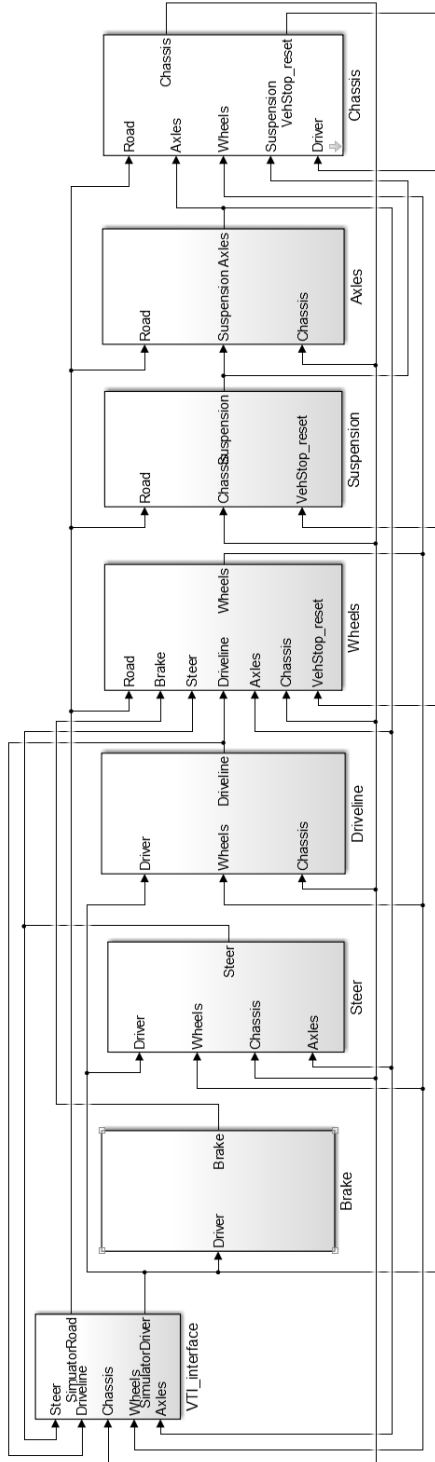


Figure 2.3: The vehicle model in Simulink.

2.2 Chassis dynamometer laboratory

To obtain model parameters such as gear ratios and engine inertias a chassis dynamometer was used. The chassis dynamometer laboratory is located at Linköping University, a picture of the chassis dynamometer laboratory can be seen in Figure 2.4.

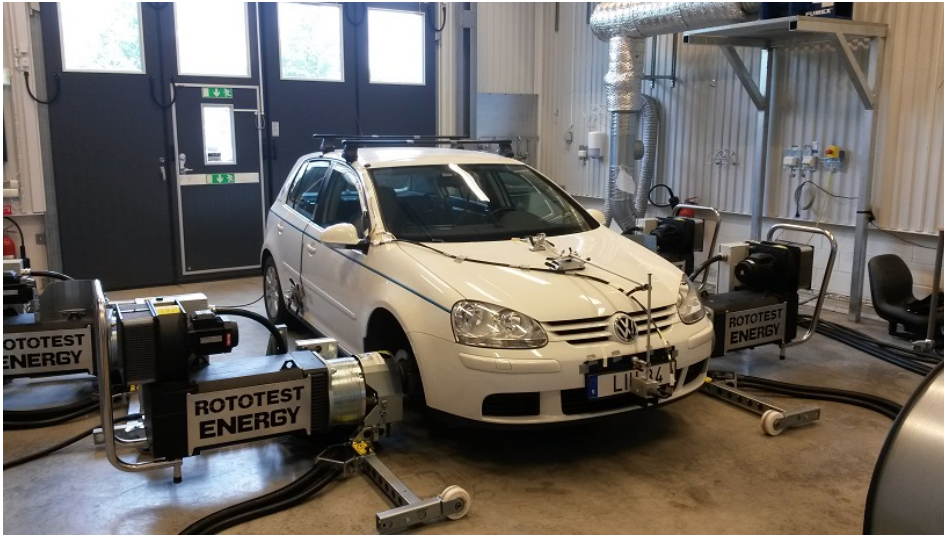


Figure 2.4: Golf V mounted to the chassis dynamometers.

The chassis dynamometer consist of four mobile dynamometer units and a mobile head wind fan. The dynamometers units can be operated as either motors or generators to brake and propel the vehicle. The dynamometers are mounted directly on the vehicles wheel hubs using adapter plates, see Figure 2.5. The head wind fan simulate the head-wind at different speeds which cools the engine and its components. The fan is capable of wind speeds up to 100 km/h according to [19], see Figure 2.6 for a picture of the fan. The chassis dynamometer outputs can be seen in Table 2.1, the highlighted outputs were used in this thesis. The wheel torque measurement accuracy is within 0.1 % of measured value according to [19].

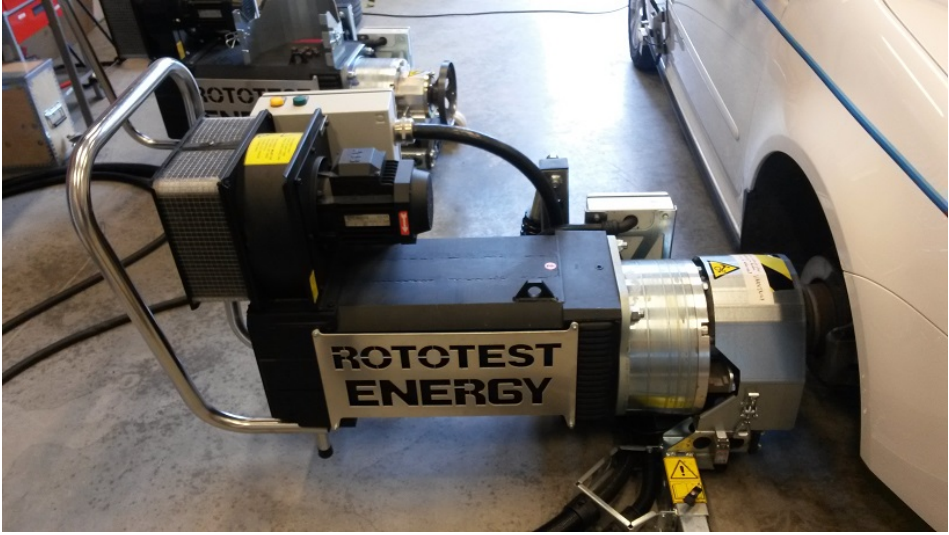


Figure 2.5: A dynamometer unit mounted to the wheel hub using a adapter plate.



Figure 2.6: Head wind fan.

| Output | Description |
|------------|---------------------------------------|
| n_i | Wheel speed for wheel i |
| M_i | Wheel torque for wheel i |
| vl | Vehicle longitudinal velocity |
| vv | Vehicle velocity |
| r_{road} | Road curvature radius |
| H | Heading, relative origin |
| h | Elevation of road |
| p | Incline |
| dTP | Distance since start |
| tTP | Time since start |
| T_i | Dynamometer temperature for wheel i |

Table 2.1: Outputs from the chassis dynamometer, the highlighted outputs in the table were used in this thesis. In the table $i = \{1, 2, 3, 4\} = \{lf, rf, lr, rr\}$ where lf is left front, rf is right front, lr is left rear and rr is right rear.

The chassis dynamometer currently has two test modes which are road resistance and constant speed. In road resistance mode the chassis dynamometer simulates the forces that the vehicle has to overcome on a road. The forces that are simulated are the aerodynamic drag force F_{air} , the rolling resistance F_{roll} and if the road is not flat the gravitational resistance F_{grav} . The driving resistances model used in the chassis dynamometer is presented in [19] and is

$$F_{res} = F_{roll} + F_{air} + F_{grav} \quad (2.1a)$$

$$F_{roll} = c_r \cdot m \cdot g \quad (2.1b)$$

$$F_{air} = \frac{1}{2} \cdot \rho_a \cdot c_d \cdot A_f \cdot (v + v_0)^2 \quad (2.1c)$$

$$F_{grav} = m \cdot g \cdot \alpha \quad (2.1d)$$

where c_r is the rolling resistance coefficient, m is the vehicle mass, g is the gravitational constant, ρ_a is the density of air, c_d is the drag coefficient, A_f is the frontal area of the vehicle, v_0 is the wind speed relative to the ground during the experiment and α is the slope of the road. During a road resistance experiment the vehicles acceleration is

$$m \cdot a = F_{prop} - F_{res} \quad (2.2a)$$

$$F_{prop} = \sum_i \frac{M_{w,i}}{r_w} \quad (2.2b)$$

where F_{prop} is the propulsion force calculated from measured torque on each driv-

ing wheel $M_{w,i}$ and the wheel radius r_w . In constant speed mode the chassis dynamometer maintains a predefined engine or wheel speed for a specific gear. The chassis dynamometer maintains the predefined speed even if the driver varies the gas pedal. For the constant speed mode the forces at the wheels are the forces needed to maintain the speed, the driving resistances forces are not simulated in this test mode.

2.3 Pedal robot

A pedal robot has been developed to connect the driving simulator at VTI with the chassis dynamometers at LiU. The pedal robot consists of two electrical linear actuators of ball screw type that is used to manipulate the pedals, see Figure 2.7 for a picture of the pedal robot. The actuators are equipped with two circuit breakers each to define the maximum and minimum position of the piston.

When using the pedal robot to connect the simulator with the dynamometers the pedal robot receives command signals from the driver in the simulator and returns status information back to the simulator software. When using the pedal robot as a standalone system it is controlled using Matlab simulink either with a connected steering wheel game controller or directly through the simulink interface. Regardless if the pedal robot is used as a standalone system or connected to the driving simulator it receives desired pedal positions as inputs. The pedal robot uses the desired pedal positions as reference values and a control circuit moves the pistons to the desired pedal positions. The measured piston position for the pedals is the outputs from the pedal robot.

The pedal robot was used in this thesis to obtain stable measurements, compared to a human driver, and to be able to gather pedal position data.

2.4 On-board diagnostics

On-board diagnostics or OBD is a vehicles self diagnostics and reporting capability. The current standard is called OBD-II and is installed in most cars and light trucks today. OBD-II provides access to the engine control unit (ECU) which contains diagnostics data and diagnostics trouble code (DTC). The DTC helps in identifying malfunctions in a vehicle. To access the diagnostics data requests should be sent to the ECU in the form of parameter identification numbers (PIDs). The OBD-II standard provides a list of PIDs but vehicle manufacturers are not required to implement all PIDs, so the amount of information available in a vehicle varies. The full list of standard OBD-II PIDs can be found online [8]. A vehicle's on-board diagnostics data can be read by connecting a reader tool to its OBD-II port usually located under the dashboard on the driver's side.



Figure 2.7: Pedal robot mounted in a vehicle instead of the driver's seat. The actuators are connected to the gas and clutch pedals. The red cable in the figure is from the OBD reader tool connected to the vehicle's OBD port.

2.5 Golf V

The vehicle used in this thesis is a front wheel drive Golf V with a 1.4 L multifuel engine with a manual gearbox. Vehicle data used in the chassis dynamometer can be found in Table 2.2 and the available PIDs in the Golf can be seen in Table 2.3, the highlighted PIDs in the table were used in this thesis. For the Golf V the user has access to raw data directly from the vehicle's ECU in the form of CAN data. The CAN data is used for validation purpose because a user normally do not have access to it.

| Parameter | Value |
|--------------------------------|----------------------|
| Weight - left front | 427 kg |
| Weight - right front | 382 kg |
| Wheel circumference | 1992 mm |
| Wheel diameter | 634 mm |
| Drive train | 2WD |
| Vehicle mass | 1380 kg |
| Frontal area of the vehicle | 2.460 m ² |
| Drag coefficient | 0.330 |
| Rolling resistance coefficient | 0.015 |

Table 2.2: Vehicle data for the Golf used in the chassis dynamometer.

| PID | Description |
|-----|---|
| 01 | Monitor status since DTCs cleared |
| 03 | Fuel system 1 and 2 status |
| 04 | Calculated Engine LOAD Value |
| 05 | Engine Coolant Temperature |
| 06 | Short Term Fuel Trim - Bank 1,3 |
| 07 | Long Term Fuel Trim - Bank 1,3 |
| 0B | Intake Manifold Absolute Pressure |
| 0C | Engine RPM |
| 0D | Vehicle Speed Sensor |
| 0E | Ignition Timing Advance for #1 Cylinder |
| 0F | Intake Air Temperature |
| 11 | Absolute Throttle Position |
| 12 | Commanded Secondary Air Status |
| 13 | Location of Oxygen Sensors |
| 15 | Bank 1 - Sensor 2 Oxygen Sensor Output Voltage / Short Term Fuel Trim |
| 1C | OBD requirements to which vehicle is designed |
| 21 | Distance Travelled While Malfunction Indicator Lamp is Activated |
| 34 | Bank 1 - Sensor 1 (wide range O2S) Oxygen Sensors Equivalence Ratio (λ) / Current |
| 51 | Fuel Type |
| 52 | Ethanol fuel |

Table 2.3: Available parameter identification numbers in the Golf. The high-lighted PIDs in the table were used in this thesis. The engine load value is the amount of air flowing through the engine as a percentage of the theoretical maximum.

3

Powertrain model

This chapter describes the powertrain model which consist of a developed engine model that is based on [23] and a driveline model based on [7].

3.1 Driveline model

In [7] a rigid driveline model is presented where the clutch, driveshaft and propeller shaft in the model are assumed to be stiff. The model consists of engine, clutch, transmission, propeller shaft, final drive and wheel subsystems that combined gives the driveline model. The subsystem equations in the model are derived using the generalized Newton's second law of motion.

In this thesis the driveline model from [7] have been modified and is modelled as

$$M_w = i_t i_f M_c - M_{loss:drv} \quad (3.1a)$$

$$\theta_e = i_t i_f \theta_w \quad (3.1b)$$

$$J_e \ddot{\theta}_e = M_e - M_c \quad (3.1c)$$

$$J_d \ddot{\theta}_w = M_w - r_w F_{res} \quad (3.1d)$$

which can be written as one single equation as

$$(J_d + i_t^2 i_f^2 J_e) \ddot{\theta}_w = i_t i_f (M_e - M_{loss:drv}) - r_w F_{res} \quad (3.2)$$

where i_t is the transmission conversion ratio, i_f is the final drive conversion ratio, M_c is the clutch torque, M_w is the wheel torque, θ_e is the angle of the engine, θ_w is the angle of the wheel, J_e is the engine inertia, $\dot{\theta}_e$ is the engine angular acceleration, M_e is the engine torque, $M_{loss:drv}$ is the driveline losses, J_d is the driveline inertia, r_w is the wheel radius and F_{res} is the driving resistance from 2.1.

The driveline losses are the friction torque losses in the driveline that are estimated from measurements performed in the chassis dynamometer. The measurements were performed with the clutch disengaged and by not moving the gas pedal, see Section 4.3 for the estimated driveline losses. The driveline losses are implemented as a map with gear and engine speed as inputs and the driveline losses as output.

The driveline inertia, J_d , is the inertias in the driveline lumped together into one inertia. The inertias in the driveline was lumped together because the inertia for each individual component can not be easily obtained. Furthermore, the driveline model used in this thesis do not require the individual inertias.

To integrate the powertrain model with the existing vehicle model the wheel torque is needed as an output. The wheel torque is used in the wheel block in the vehicle model to calculate the wheel rotation using the rolling resistance, braking torque, the wheel force and the driveline inertia. The aerodynamic drag force and the gravitational force is also calculated in the vehicle model. Because the driving resistances is handled in the existing vehicle model the implemented driveline model uses 3.1a-3.1c. However, equation 3.2 is used to estimate the inertias in Section 4.2.

3.2 Engine model

In [23] performance maps are used to get steady state values of the engine. The same concept is used in this thesis to develop two static maps, a pedal map and an engine map. The pedal map is created using the fact that a constant pedal position and engine speed gives a constant throttle position. The engine map is created in similar manner using that a constant throttle position and engine speed gives a constant engine torque. The maps are connected to each other in series as in Figure 3.1.

With the throttle position available from the OBD in the Golf V, see Table 2.3, two maps were created to investigate them separately. However if the throttle position is not available in a vehicle it is possible to use one static map with pedal position and engine speed as input and engine torque as output.

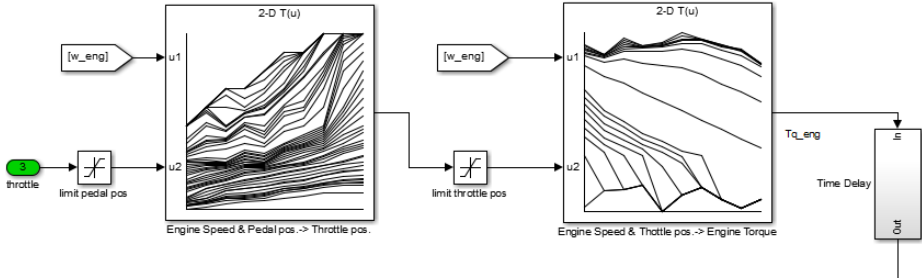


Figure 3.1: Pedal map and engine map connected in series with a first order lag element as a time delay. The pedal map uses the engine speed and pedal position, called w_eng and throttle (as in throttle pedal) respectively in the figure, as inputs with throttle position as output. The engine map uses the engine speed and throttle position as inputs and engine torque as output.

The maps were created using the constant speed test mode in the chassis dynamometer. In a constant speed test the chassis dynamometer tries to maintain a predefined engine/wheel speed even when the driver moves the gas pedal. By holding the engine speed fixed and performing measurements on different pedal positions static maps were obtained. The engine torque was chosen as output for the engine model so that the engine and driveline models can be linked together. See Section 4.4 for a more detailed description on how the maps were estimated.

Because the maps were created using static measurements they lack dynamics. To add dynamics to the maps a time delay is used in the powertrain model. The time delay is for the delay from a change in pedal position to a change in wheel torque.

In [23] a first order lag element is used to model a time delay from the injected fuel to a change in engine torque for a four-stroke cycle six cylinder high speed engine. The time constant for the lag element in [23] is dependent on the engine speed. The powertrain model in this thesis uses the same concept to model the time delay from a change in pedal position to a change in wheel torque. However from step response tests performed with the Golf V it was determined that the time constant in this case was not dependent on the engine speed. The time delay in the powertrain model is modelled as

$$M_{e,delay} = \frac{1}{\tau_c s + 1} M_{e,stat} \quad (3.3)$$

where τ_c is the time constant, $M_{e,stat}$ is the engine torque from the static maps and $M_{e,delay}$ is the delayed engine torque. The time constant τ_c was estimated from test data, see Section 4.5 for more details.

The engine speed in the model is calculated from the wheel speeds according to 3.1b. However if the clutch is disengaged or if the gearbox is in neutral the engine speed can not be calculated from the wheel speed correctly. For the above mentioned cases where the engine is not connected to the driveline and runs freely the engine speed is calculated from the engine torque using 3.1c and considering that $M_c = 0$, which results in

$$\dot{\theta}_e = \int \frac{M_e}{J_e} dt \quad (3.4)$$

The implementation of the engine speed calculation, from the wheel speed according to 3.1b and from the engine torque according to 3.4, can be seen in Figure 3.2. In the figure the soft switch block handles the switch between the two calculations with the help of the clutch signal. The switch can be described as

$$\dot{\theta}_e = \dot{\theta}_{e,int}(1 - \delta_{cl}) + \dot{\theta}_{e,wh}\delta_{cl} \quad (3.5)$$

where $\dot{\theta}_{e,int}$ is the angular velocity of the engine calculated from the engine torque, $\dot{\theta}_{e,wh}$ is the angular velocity of the engine calculated from the wheel speed and δ_{cl} is the clutch signal. The clutch signal is a value between 0 and 1 where 0 represent that the pedal is in its bottom position and 1 represent that the pedal is in its top position. However when the transmission is in neutral gear the engine speed is always calculated from the engine torque. See Figure 3.3 for a image of the implemented soft switch in Simulink.

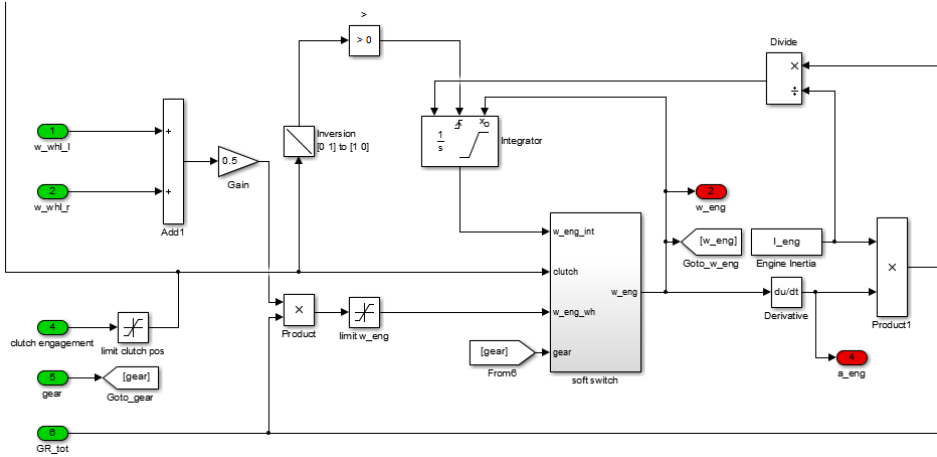


Figure 3.2: Engine speed calculations for the powertrain model implemented in Simulink. The soft switch block handles the switch between engine speed calculation sources when the clutch is disengaged.

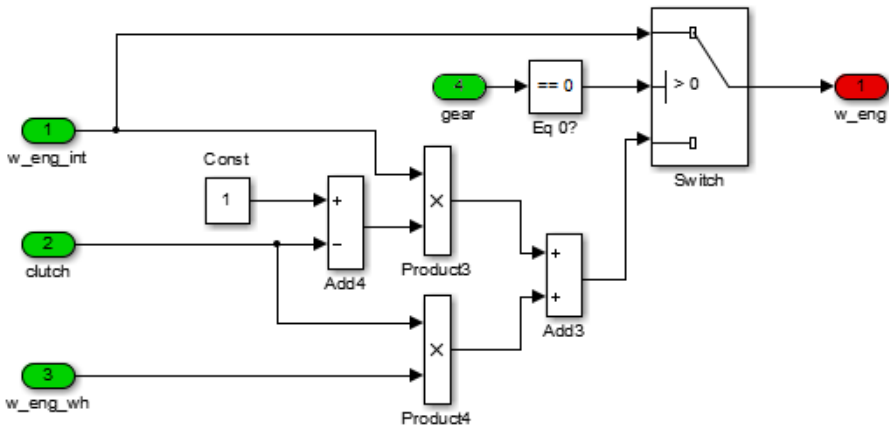


Figure 3.3: Soft switch subsystem block where the switch between engine speed calculation sources is performed. w_{eng_int} is the engine speed calculated from the engine torque using a integral and w_{eng_wh} is the engine speed calculated from the wheel speed.

The clutch signal is also used to gradually set the driveline torque to zero when the clutch is disengaged, see Figure 3.4. If a driver switch gears without pressing down the clutch pedal the driveline torque will switch instantly to zero between gears. This is because between gears the gear signal is zero and the driveline torque is calculated from the combined gear and final drive ratio which is zero for neutral. This will cause problems when the model is used in the driving simulator with movement. To prevent the instantaneous switch to zero a logic circuit is implemented that uses a lag element to slowly decrease down to zero if the gear is changed to neutral without disengaging the clutch, see Figure 3.4. In first gear there are large negative spikes when the vehicle starts from standing still and when gear-shifting down. To remove the negative spikes a logic circuit that sets the driveline torque to zero when the model is in 1st gear and the engine torque is negative is implemented, see Figure 3.4.

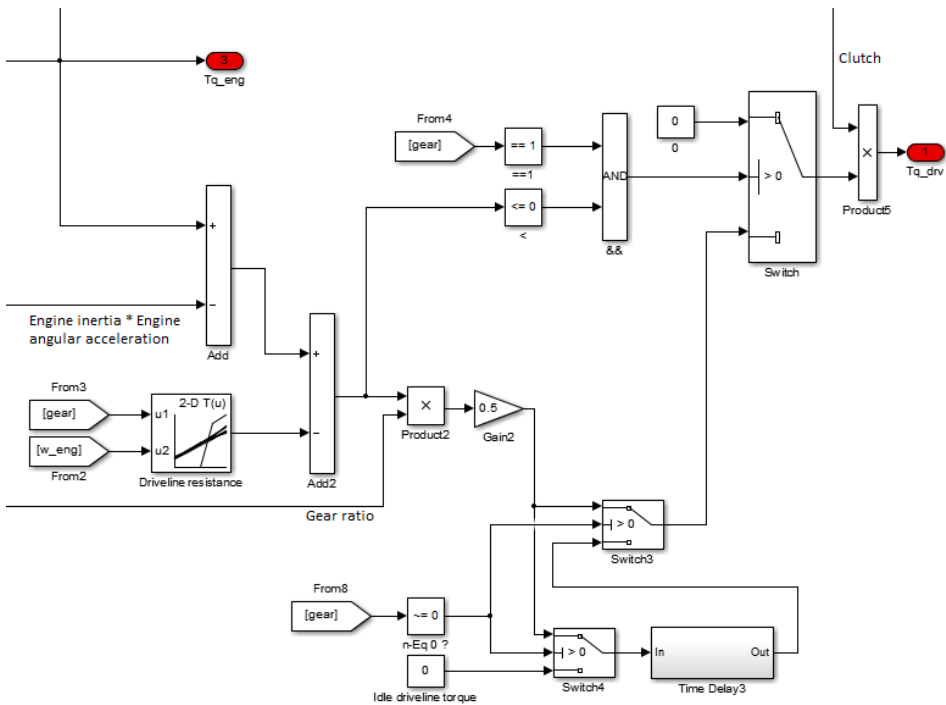


Figure 3.4: Driveline and engine torque outputs from the powetrain model implemented in Simulink. Two logic circuits are used in the model one to prevent sudden switches to zero driveline torque, if the driver changes gear by disengaging the clutch, and one to prevent negative spikes in first gear.

3.3 Engine loss model

To investigate the effects of the engine losses in the engine map an engine loss model is used. The engine loss model and its submodels used in this thesis is presented in [7]. The engine torque is modelled as

$$M_e = \frac{W_{i,g} - W_{i,p} - W_{fr}}{2n_r\pi} \quad (3.6)$$

where M_e is the engine torque, $W_{i,g}$ is the gross indicated work, $W_{i,p}$ is the pumping work and W_{fr} is the engine friction. The engine loss can be calculated from the engine torque model by performing a measurement while not pressing the gas pedal. By not pressing the gas pedal no fuel is injected into the engine and because the gross indicated work is coupled to the energy that comes from the delivered fuel, the gross indicated work is zero for the measurement. With zero gross indicated work 3.6 is

$$M_e = \frac{W_{i,g} - W_{i,p} - W_{fr}}{2n_r\pi} \xrightarrow{\{W_{i,g}=0\}} M_e = \frac{-W_{i,p} - W_{fr}}{2n_r\pi} \quad (3.7)$$

The pumping work is modelled as

$$W_{i,p} = V_D \cdot (p_{em} - p_{im}) \quad (3.8)$$

where V_D is the engine displacement volume, p_{em} and p_{im} are the exhaust and intake manifold pressure. The engine friction is modelled as

$$W_{fr} = V_D \cdot FMEP \quad (3.9a)$$

$$FMEP = \xi_{aux} \cdot [(0.464 + 0.0072 \cdot S_p^{1.8}) \cdot \Pi_{bl} \cdot 10^5 + 0.0215 \cdot BMEP(p_{im})] \cdot \left(\frac{0.075}{B}\right)^{0.5} \quad (3.9b)$$

$$S_p = 2 \cdot S \cdot \frac{\dot{\theta}_e}{60} \quad (3.9c)$$

where ξ_{aux} is the load from the auxiliary devices, S_p is the mean piston speed, S is the engine piston stroke, Π_{bl} is the boost layout (an engine without a turbo has $\Pi_{bl} = 1$), $BMEP$ is the brake mean effective pressure and B is the engine bore.

The brake mean effective pressure is modelled as

$$BMEP(p_{im}) = -C_{p1} + C_{p2} \cdot p_{im} \quad (3.10a)$$

$$M_e(p_{im}) = \frac{BMEP(p_{im})V_D}{n_r 2\pi} \quad (3.10b)$$

where n_r is the number of engine revolutions per cycle and C_{p1} and C_{p2} were estimated from measurement data. The engine losses for the Golf V and its effects on the engine map can be seen in Section 4.3.

4

Parametrization methodology

This chapter describes how the powertrain model parameters were estimated and how the tests to estimate the parameters were designed.

4.1 Combined gear and final drive ratios

The combined gear and final drive ratio $i_t i_f$ was estimated by performing constant speed tests in the chassis dynamometer for each gear. This is due to the wheel speed being proportional to the engine speed by the ratio for each gear as 3.1b which is

$$\dot{\theta}_e = i_t i_f \dot{\theta}_w$$

where $\dot{\theta}_w$ and $\dot{\theta}_e$ is the wheel and engine angular velocity respectively. From engine and wheel speed data the ratios were estimated by method of least squares. In Figure 4.1 a constant speed test has been performed for 3rd gear at 2500 RPM engine speed and it was used to validate the estimated ratios by comparing the calculated engine speed from the wheel speed with the measured engine speed. A histogram plot of the error $e = \dot{\theta}_e - i_t i_f \dot{\theta}_w$ can be seen in Figure 4.2. The data in Figures 4.1 and 4.2 were from a validation dataset, i.e., not the same dataset that were used to estimate the ratios. From Figure 4.1 it can be observed that the calculated engine speed is slightly higher than the measured engine speed which coincide with the mean value of the distribution of the error in Figure 4.2, which is around -9 RPM. The measurement is for an engine speed of 2500 RPM which means that the error is relatively small and the ratio gives good results. The estimated ratios for the Golf V can be found in Table 4.1.

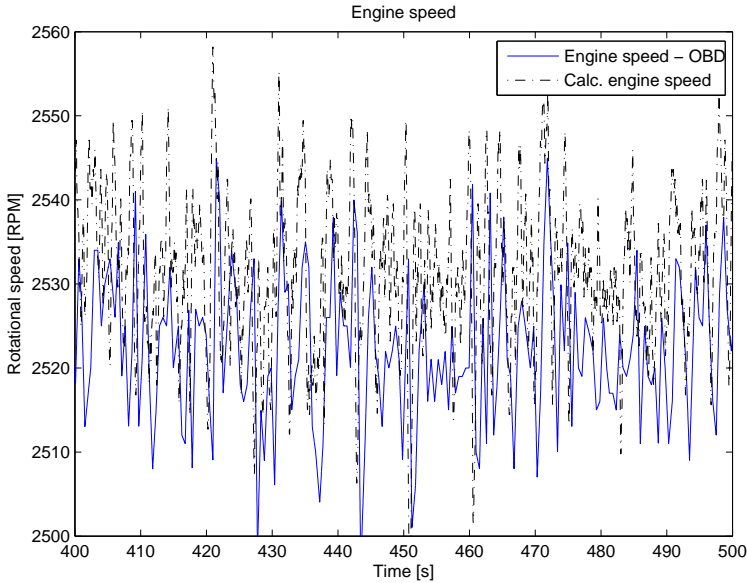


Figure 4.1: Comparison view of the calculated engine speed and the measured engine speed from the OBD for a constant speed test for 3rd gear at 2500 RPM engine speed. The black dash-dotted line in the figure is the calculated engine speed using the wheel speed from the chassis dynamometer and the estimated ratios.

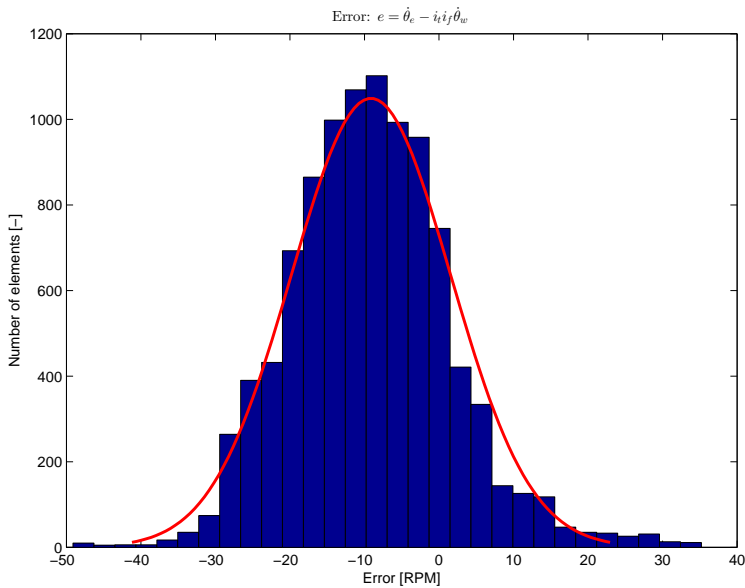


Figure 4.2: Histogram plot of the error $e = \hat{\theta}_e - i_t i_f \hat{\theta}_w$ with a normal distribution fit (red curve).

| Gear [-] | Ratio [-] |
|----------|-----------|
| 1st | 15.72 |
| 2nd | 8.90 |
| 3rd | 5.83 |
| 4th | 4.44 |
| 5th | 3.70 |

Table 4.1: Estimated combined gear and final drive ratios for the Golf V.

4.2 Driveline and engine inertia

The engine and driveline inertia of the Golf V were estimated with the help of the chassis dynamometer and 3.2. Constant speed test mode was used in the chassis dynamometer to estimate the inertias. In 3.2 it can be observed that the inertia of the powertrain is $J_{pwr} = (J_d + i_t^2 i_f^2 J_e)$ where J_d is the driveline inertia and J_e is the engine inertia. This means that two measurement sets had to be logged, one with the clutch engaged to estimate the powertrain inertia and one with the clutch disengaged to estimate the driveline inertia. The engine inertia was then estimated with the help of the combined gear and final drive ratios from Section 4.1.

During the measurements data was logged from the chassis dynamometer and the OBD port. The OBD PIDs used for the measurements are engine speed, air/fuel ratio (lambda), throttle position and intake manifold pressure. The intake manifold pressure was not used to calculate the inertias but the test data was used to estimate the engine and driveline losses in Section 4.3.

To get a correct estimate of the powertrain inertia from the measurements the engine was not allowed to generate any torque. To prevent the engine from generating any torque the gas pedal was not moved during the measurements. To make sure that the engine did not generate any torque the air/fuel ratio (lambda) was used to check if any fuel was injected during the measurements. A lambda of 2 indicates that no fuel is injected and only air passes through the engine.

The inertias was estimated using 3.2 where the torque in the right hand side is the wheel torque required to accelerate the powertrain. However the air/fuel ratio for low engine speeds was not 2 even when the gas pedal was not moved. This meant that the measurements had to start from an engine speed where the air/fuel ratio was 2. To obtain the wheel torque required to accelerate the powertrain/driveline when the measurements have a starting engine speed the steady state friction torque had to be removed. Equation 3.2 is written as

$$(J_d + J_e i_t^2 i_f^2) \ddot{\theta}_w = M_{w,Dyn} - M_{fric}(\dot{\theta}_w) = M_{acc,pwr} \quad (4.1)$$

when the clutch is engaged and

$$J_d \ddot{\theta}_w = M_{w,Dyn} - M_{fric}(\dot{\theta}_w) = M_{acc,drv} \quad (4.2)$$

when the clutch is disengaged, where $M_{w,Dyn}$ is the wheel torque from a dynamic measurement, $M_{fric}(\dot{\theta}_w)$ is the steady state friction torque for wheel speed $\dot{\theta}_w$ and $M_{acc,pwr}/M_{acc,drv}$ is the wheel torque required to accelerate the powertrain/driveline. The M_{fric} is a map of the steady state friction torque obtained from constant speed measurements for engine speed from 1000 RPM to 5000 RPM with steps of 500 RPM. In Figures 4.3 and 4.4 constant speed measurements have been performed for 5th gear both with the clutch engaged and disengaged.

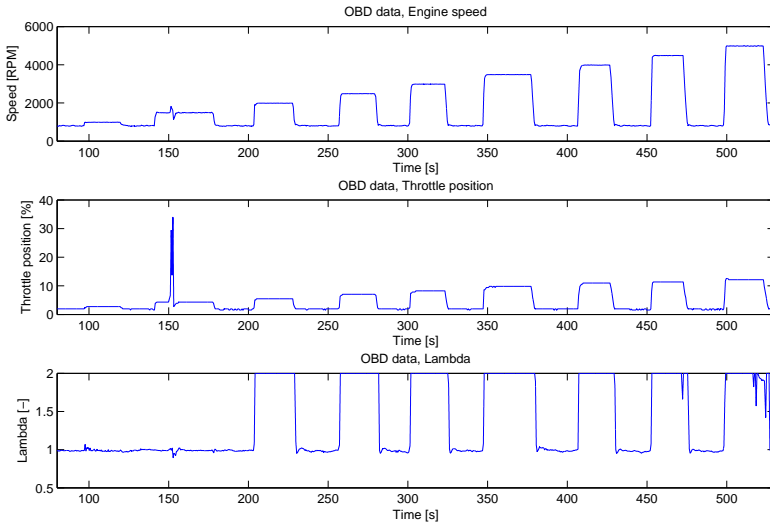


Figure 4.3: OBD data for a constant speed measurement for 1000 RPM to 5000 RPM with steps of 500 RPM engine speed for 5th gear. For engine speeds over 1500 RPM the air-fuel ratio, lambda, is two which means that no fuel is injected in the engine. All engine speed measurement points are done first with the clutch disengaged and then the clutch engaged.

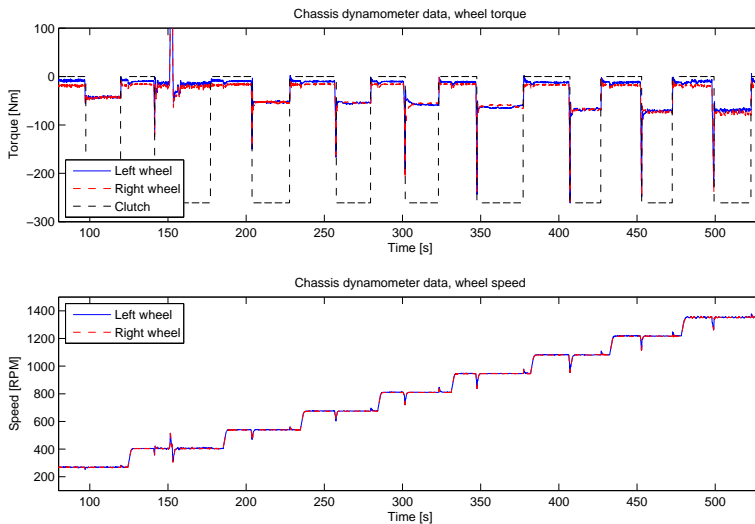


Figure 4.4: Chassis dynamometer data for a constant speed measurement for 1000 RPM to 5000 RPM engine speed with steps of 500 RPM for 5th gear. The black dashed line in the torque plots is the clutch signal where 0 is disengaged clutch and non zero is engaged clutch. All engine speed measurement points are done first with the clutch disengaged and then the clutch engaged.

From the constant speed measurement data a static map was created which can be seen in Figure 4.5. In the figure it can be observed that the friction torque for a wheel speed of 400 RPM gave inconsistent values, for 5th gear a wheel speed of 400 RPM is equal to an engine speed of 1500 RPM. However the lambda values in Figure 4.3 for an engine speed of 1500 RPM indicated that combustion was taking place and it was therefore not used in the dynamic measurement. The dynamic measurement was performed by changing operating point during a constant speed measurement from an engine speed of 2000 RPM to 4000 RPM and back again for 5th gear where the lambda value was 2. The dynamic measurement can be seen in Figures 4.6 and 4.7.

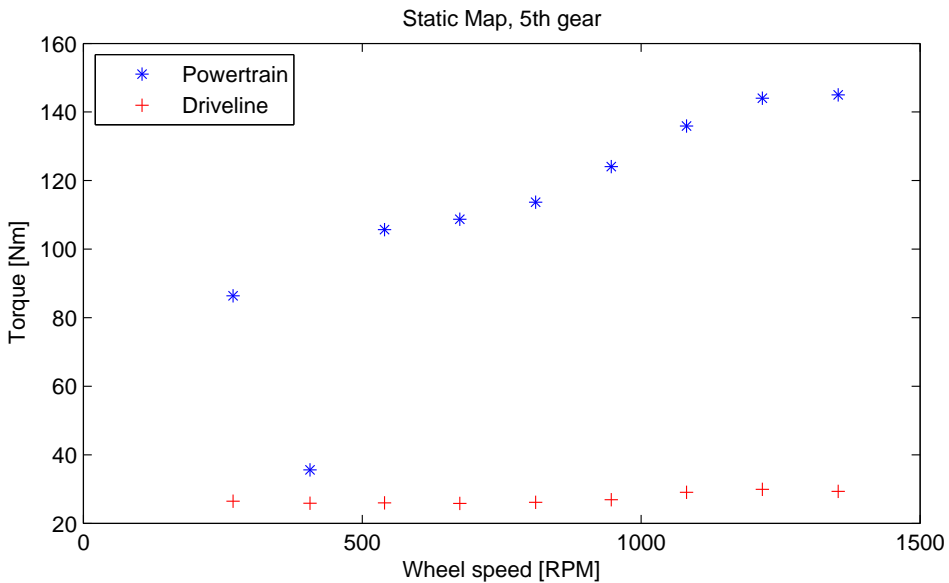


Figure 4.5: Map of the steady state friction torque for 5th gear. The friction torque for wheel speed of 400 RPM gave inconsistent values due to problems during the measuring. However the lambda values in Figure 4.3 for an engine speed of 1500 RPM indicated that combustion was taking place and it was therefore not used in the dynamic measurement.

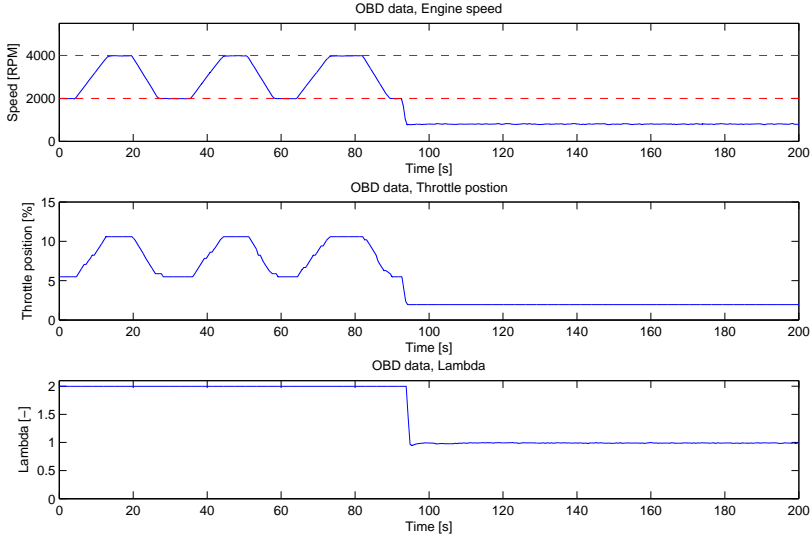


Figure 4.6: OBD data for a dynamic measurement with steps in engine speed from 2000 RPM up to 4000 RPM for 5th gear and back again done 3 times each for engaged and disengaged clutch. During disengaged clutch the engine speed is the engine idle speed. The air/fuel ratio, lambda, is two during the test which means that no fuel is injected in the engine.

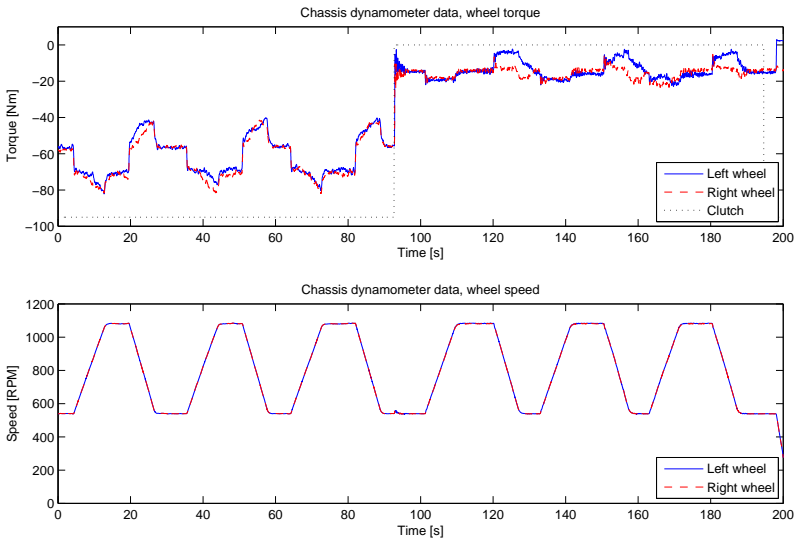


Figure 4.7: Chassis dynamometer data for a dynamic test with steps in engine speed from 2000 RPM up to 4000 RPM for 5th gear and back again done 3 times each for engaged and disengaged clutch. The black dashed line in the torque plots is the clutch signal where 0 is disengaged clutch and non zero is engaged clutch.

The resulting wheel torques required to accelerate the powertrain and the driveline can be seen in Figure 4.8. The figure also contains the angular acceleration of the wheel for the powertrain and the driveline. The angular acceleration of the wheel was estimated by differentiating the wheel speed. The estimated angular acceleration was very noisy so a spectral analysis was performed to analyse the energy content of the signal, see Figure 4.9. In the figure it can be observed that the energy content of the data is at low frequencies, so a low pass filter was designed to reduce the noise. The red curve in Figure 4.8 is the low pass filtered angular acceleration of the wheel using a second order Butterworth filter with a cutoff frequency of 1.5 Hz.

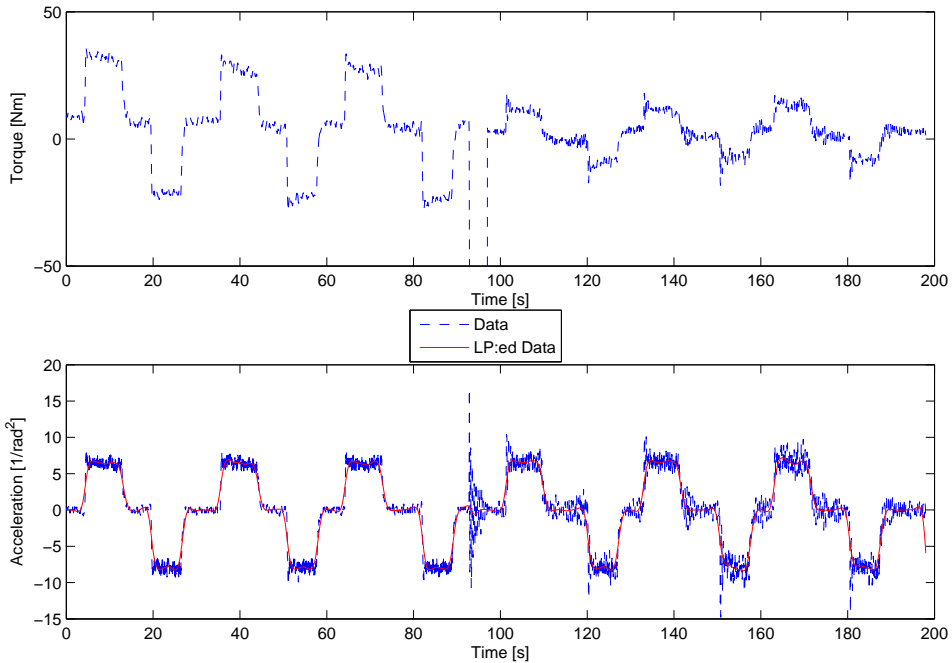


Figure 4.8: The resulting wheel torques required to accelerate the powertrain ($M_{acc,pwr}$) and the driveline ($M_{acc,drv}$) for 5th gear with its corresponding wheel acceleration. The three first steps from 0 s to 90 s is for the powertrain and the three last steps from 100 s to 200 s is for the driveline. The red curve in the angular acceleration plot is the low pass filtered data using a second order Butterworth filter.

The inertias was then estimated from the measurement data in Figure 4.8 and equations 4.1 - 4.2 by method of least squares. The powertrain inertia for a step at 65 s to 71 s and the driveline inertia for a step at 164 s to 170 s in Figures 4.6-4.8 can be seen in Figure 4.10. The red lines in the figure is the powertrain and driveline inertias from method of least squares. The estimated engine inertia from the driveline and powertrain inertias in Figure 4.10 using $J_e = (J_{pwr} - J_d)/i_t^2 i_f^2$ and $i_t i_f$ for 5th gear from Table 4.1 was 0.166. For the three steps in Figure 4.8 the engine inertias were 0.186, 0.238 and 0.166 which gives a mean value of 0.197. The driveline inertia in the figure were 1.734, 1.689 and 2.004 which gives a mean value of 1.8094.

With the estimated engine and driveline inertias the left and right hand sides of 4.1 and 4.2 can be compared to evaluate the estimated inertias, see Figure 4.11 for comparison plots. In the figure it can be observed that the result have a slight error but overall the curves match for acceleration steps but not for deceleration steps. This is because the inertias have been estimated from data for acceleration steps. If the inertias are estimated from data for deceleration steps they will be lower than when they are estimated from an acceleration step. In Figure 4.12 the errors $e = M_{acc,drv} - J_d \ddot{\theta}_w$ and $e = M_{acc,pwr} - J_{pwr} \ddot{\theta}_w$ are presented as histogram plots. The error plots shows that both the powertrain and driveline have an error which was visible in the comparison plots.

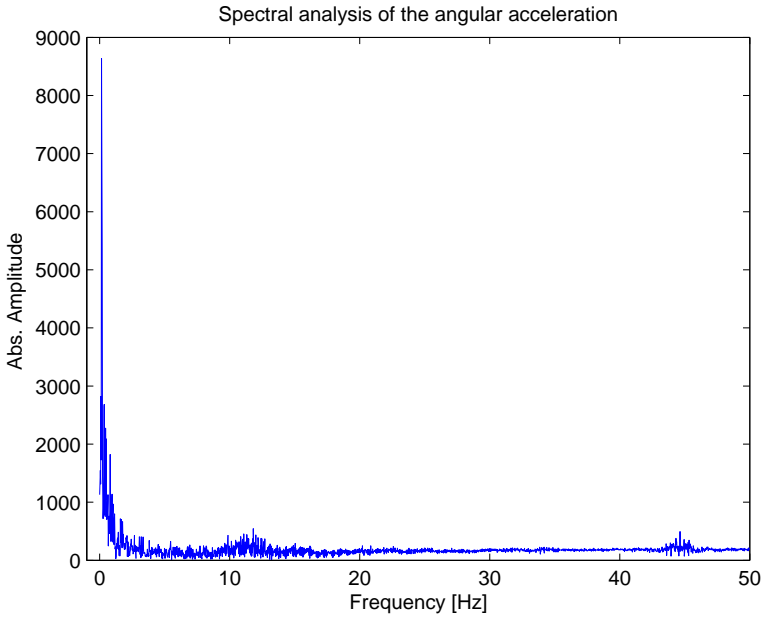


Figure 4.9: Spectral analysis of the angular acceleration of the wheel.

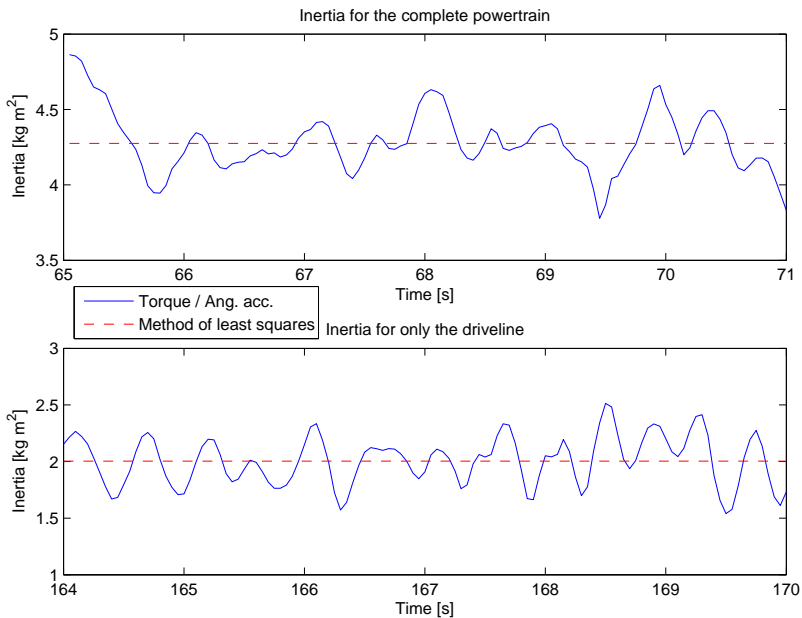


Figure 4.10: The blue curve is powertrain and driveline inertias for a step in engine speed by dividing the torque with the angular acceleration from Figure 4.8. The red line is the powertrain and driveline inertias from method of least squares.

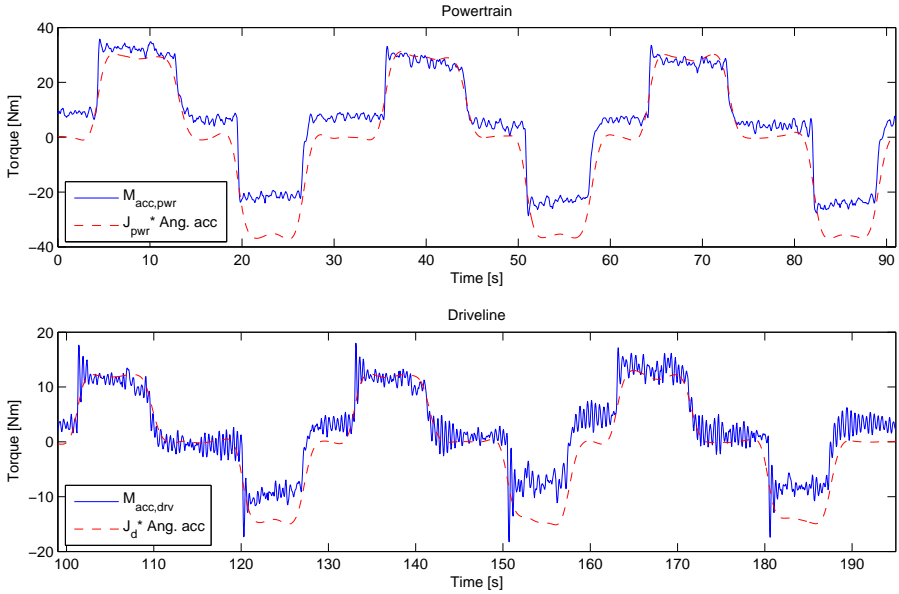


Figure 4.11: Top plot is a comparison plot of $M_{acc,pwr}$ (blue curve) and $J_{pwr}\ddot{\theta}_w$ (red curve). Bottom plot is a comparison plot of $M_{acc,drv}$ (blue curve) and $J_d\ddot{\theta}_w$ (red curve).

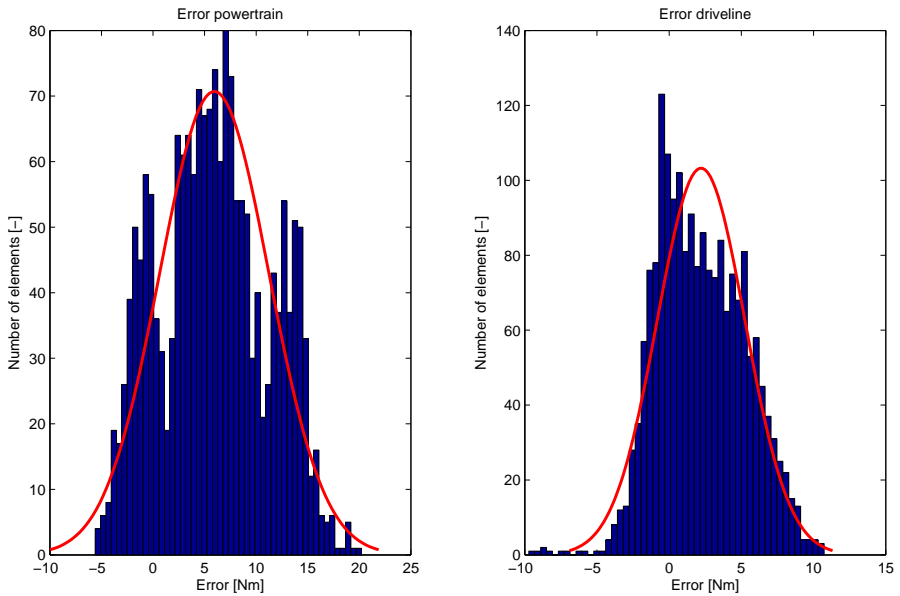


Figure 4.12: Histogram plots of the errors $e = M_{acc,pwr} - J_{pwr}\ddot{\theta}_w$ for the powertrain and $e = M_{acc,drv} - J_d\ddot{\theta}_w$ for the driveline with normal distribution fit (red curve).

4.2.1 Alternative method: Engine inertia

If a test vehicle has the engine torque PID available from the OBD, the engine inertia can be obtained by performing an idle engine test. In the Golf the engine torque is available from the CAN data, so to validate the estimated engine inertia from Section 4.2 an idle engine test was performed. During the idle engine test CAN data were logged for engine speed and engine torque. The inertia was then calculated using the generalized Newton's second law of motion

$$M = J\ddot{\theta} \quad (4.3)$$

where M is the torque, J is the inertia and $\ddot{\theta}$ is the angular acceleration. The engine speed was differentiated to obtain the angular acceleration of the engine. The calculated angular acceleration was very noisy so a spectral analysis was performed to analyse the energy content of the signal. The spectral analysis was then used to design a filter to remove the noise. See Figure 4.13 for plots of engine angular velocity, torque and angular acceleration data for an idle engine test and a spectral analysis of the acceleration data.

In the spectral analysis plot in Figure 4.13 the energy content of the data is at low frequencies so a low pass filter was designed to reduce the noise. The red curve in the plot of the angular acceleration is low pass filtered data using a second order Butterworth filter with a cutoff frequency of 1.5 Hz. The engine inertia was estimated by method of least squares from the filtered acceleration data and the engine torque. In Figure 4.14 the engine inertia for the step in Figure 4.13 is presented, the red line in the figure is the engine inertia from method of least squares. The engine inertia was 0.196 which is close to the to the estimated engine inertia from Section 4.2 which was 0.197.

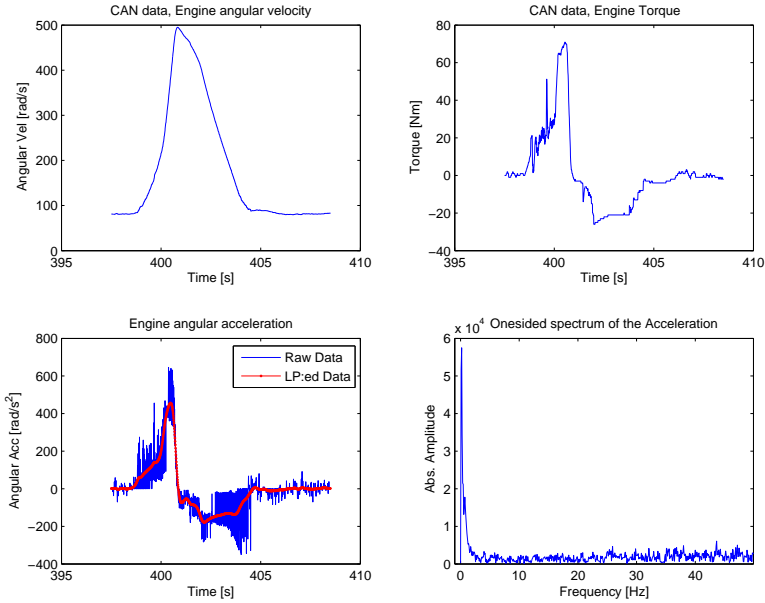


Figure 4.13: Engine angular velocity, torque, angular acceleration and a spectral analysis of an idle engine test. The red curve in the acceleration plot is low pass filtered data using a second order Butterworth filter.

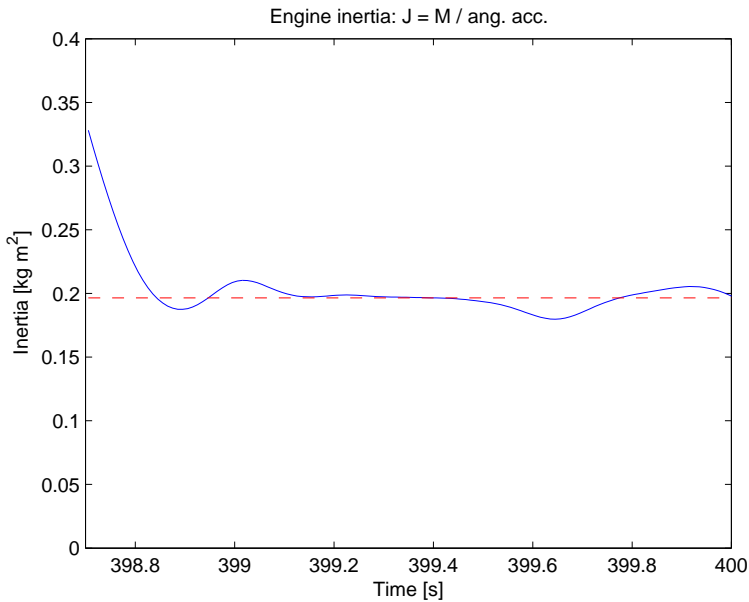


Figure 4.14: The blue curve is engine inertia for a step in engine speed by dividing the torque with the angular acceleration from Figure 4.13. The red line is the engine inertias from method of least squares.

4.3 Driveline and engine losses

The engine map used in the engine model was created using measurements performed in a specific gear and engine speed, see Section 4.4 for more details on how the map was created. For example the engine torque in the engine map for an engine speed of 1500 RPM were created from measurements performed in 4th gear. However the engine map is used in the powertrain model to calculate the wheel torque for all gears. This means that gear dependent losses in the powertrain may impact the results when the engine torque from the engine map was used to calculate the wheel torque for a different gear than it was created with, for example 3rd gear for an engine speed of 1500 RPM. To compensate for this a loss model was included in the powertrain model. To determine what losses are gear dependent the driveline and engine losses are estimated. The driveline and engine losses were estimated from the data collected for the inertias in section 4.2. The driveline losses were estimated as

$$M_{loss:drv} = -\frac{M_{w,right} + M_{w,left}}{i_t i_f} \quad (4.4)$$

using the data collected for the inertias in Section 4.2 where the clutch was disengaged. When the clutch is disengaged the wheel torque from the chassis dynamometer is the friction torque needed to rotate the driveline. The estimated driveline friction losses for each gear can be seen in Figure 4.15. For measurement with the clutch disengaged the difference in wheel torque for the different engine speeds are very small which can be observed in Figure 4.4. With small differences in the wheel torque the mean value of the measurements are sensitive to noise. This may explain why the values for 5th gear for 4000 RPM - 5000 RPM engine speed are slightly higher than the rest of the values for 5th gear.

As the gas pedal was untouched during the measurements the engine losses from the loss model can be calculated from 3.6 - 3.10. Specification is for the engine such as piston stroke, engine bore and engine displacement volume for the Golf V can be found online [2]. For the pumping work in 3.8 the exhaust manifold pressure was approximated to the ambient air pressure because it is not available from the OBD for the Golf V. The intake manifold pressure on the other hand is available from the OBD and was logged during the measurements.

For the engine friction in 3.9 according to [7] the load from the auxiliary devices are approximately 1.3 - 1.4. The engine do not have a turbo so the boost layout is 1. For the brake mean effective pressure 3.10a and 3.10b are combined to

$$M_e(p_{im}) = \frac{V_D}{n_r 2\pi} \cdot (-C_{p1} + C_{p2} p_{im}) = \frac{V_D}{n_r 2\pi} \cdot \begin{bmatrix} -1 & p_{im} \end{bmatrix} \begin{bmatrix} C_{p1} \\ C_{p2} \end{bmatrix} \quad (4.5)$$

where C_{p1} and C_{p2} were estimated from the collected intake manifold and the engine torque data using method of least squares. The resulting engine loss calculated from 3.6 - 3.10 for data from each gear can be seen in the plot to the left in Figure 4.16. From the figure it can be observed that the engine losses are not dependent on the gear and if this is the case then adding the engine losses to the powertrain model is redundant. This is because the engine map contains the engine losses for the gear it was created in and if the engine losses are the same for all gears there is no need to compensate for another gear. To verify this the engine losses were estimated from the chassis dynamometer data as

$$M_{loss:eng} = -\frac{M_{w,right} + M_{w,left}}{i_t i_f} - M_{loss:drv} \quad (4.6)$$

using the data collected for the inertias in Section 4.2 where the clutch was engaged. When the clutch is engaged the wheel torque from the chassis dynamometer is the friction torque needed to rotate the powertrain. However to get the correct friction torque from the measurements the engine was not allowed to generate any torque which means that the lambda value had to be 2. A lambda of 2 indicates that no fuel is injected and only air passes through the engine. This was not the case for 1000 RPM and 1500 RPM engine speed for all gears. Furthermore the wheel torque for 3rd, 4th and 5th gear for an engine speed of 1500 RPM was incorrect due to problems during the measurements. As such only engine speed from 2000 RPM and higher is of interest in the plot to the right in Figure 4.16. For engine speeds from 2000 RPM and above the losses are close to each other except for some values for 1st gear that are 0.5 - 1.5 Nm from the rest. This indicates that the engine losses are not dependent on the gear. With both the engine loss model and 4.6 indicating that the engine losses are not dependent on the gear the engine loss model is not implemented in the powertrain model. Because the engine loss model would only add and subtract the same value to the engine torque for each gear as the engine losses are the same for all gears.

As the engine losses are not gear dependent the loss model consists of the driveline losses. The loss model was implemented in two places, in the calculation of the wheel torque, as $M_{loss:drv}$ in 3.1, in the driveline model and in the estimation of the engine torque for the engine map, as $M_{loss:drv}$ in 4.7. This means that the driveline losses for the measurements used to estimate the engine torque for the engine map was added to the engine torque. For example the estimation of the engine torque for an engine speed of 1500 RPM were from measurements performed in 4th gear which means that a driveline loss of approximately 5.6 Nm, see Figure 4.15, was added to the engine torque. In the wheel torque calculation the driveline losses was then used to subtracts the losses for the gear used in the calculation. For example if the wheel torque are calculated for an engine speed of 1500 RPM and 3rd gear then approximately 4.5 Nm, see Figure 4.15, are subtracted from the engine torque.

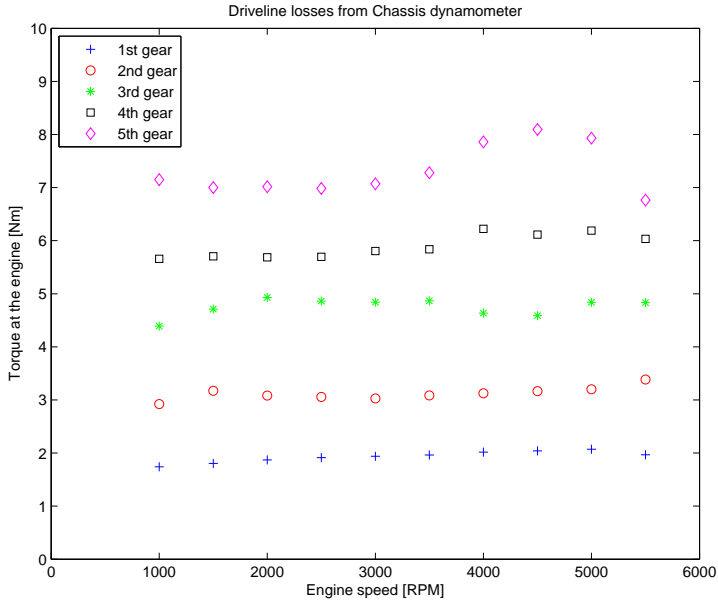


Figure 4.15: Plot over the estimated driveline friction losses for each gears using 4.4 and chassis dynamometer data. The losses in the figure is the driveline friction torque at the engine.

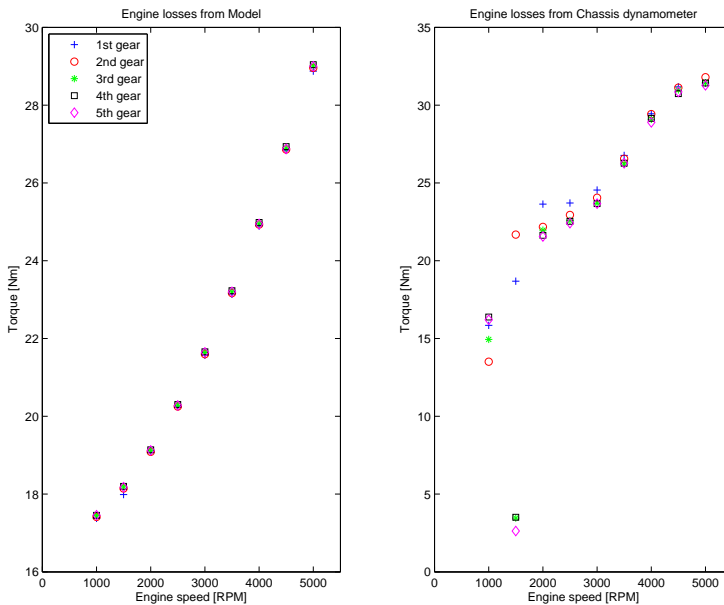


Figure 4.16: The left plot is the estimated engine losses for each gears from the engine loss model. The right plot is the estimated engine losses for each gears using 4.6 and chassis dynamometer data.

4.4 Engine and Pedal maps

The engine and pedal maps used in the engine model were estimated by performing constant speed tests in the chassis dynamometer. The engine map uses throttle position and engine speed as input and engine torque as output. The throttle positions and engine speeds used in the map can be seen in Table 4.2 and Table 4.3.

| | | | | | | | | | |
|----|----|----|----|----|----|----|----|-----|---|
| 4 | 5 | 7 | 8 | 9 | 10 | 11 | 12 | 13 | ← |
| 20 | 30 | 40 | 50 | 60 | 70 | 80 | 90 | 100 | |

Table 4.2: Throttle positions [%] used in the engine map.

| | | | | | | | | | |
|------|------|------|------|------|------|------|------|------|------|
| 1500 | 2000 | 2500 | 3000 | 3500 | 4000 | 4500 | 5000 | 5500 | 6000 |
|------|------|------|------|------|------|------|------|------|------|

Table 4.3: Engine speeds [RPM] used in the engine map.

The minimum engine speed for the map was chosen as 1500 RPM because it was the lowest engine speed the chassis dynamometer could handle. For lower engine speeds the wheel speed in the chassis dynamometer is too low and it can not rotate the wheels. The maximum engine speed was chosen as 6000 RPM by tests on the vehicle.

The map has a narrower distribution of values for lower throttle positions. Each value under 20 % in Table 4.2 corresponds to a throttle position when the gas pedal is untouched for different engine speeds. For example at 1500 RPM when the gas pedal is untouched the throttle position is approximately 4 %, at 2000 RPM the throttle position is approximately 5% and so on. The throttle position values for when the gas pedal is untouched is needed in the map to get a correct idle engine torque.

All engine speeds can not reach the higher throttle positions, for example at 2500 RPM the maximum throttle position from the engine is approximately 70 %. Empty elements in the engine map are filled with linearly extrapolated values to get a square matrix. The extrapolated values are however not used because the pedal map determines in what area of the engine map to operate in by limiting the inputs to the engine map. For example for 2500 RPM the output of the pedal map will be between 8 % and 70 % throttle position which means that the throttle position for the engine map will be between 8 % and 70 % throttle.

In Figure 4.17 a measurement series for 2500 RPM is presented. In the figure it can be estimated that the idle throttle position at 2500 RPM is approximately 8 % and throttle position for maximum gas is almost 70 %. In between the values measurements are done for 10, 20, 30, ..., 70 % throttle position. Measurements for 11, 12 and 13 % throttle positions were performed in a separate measurement set. In Figure 4.18 the throttle position, engine torque and wheel torques for 30 % throttle position, from the same measurement set as Figure 4.17, is presented.

The engine torque was calculated from the wheel torques using 3.1 and that the wheel angular acceleration for a static measurement is $\ddot{\theta}_w \approx 0$ which gives

$$\begin{aligned} J_e \ddot{\theta}_e &= M_e - M_c - M_{loss:drv} \xrightarrow{\{\ddot{\theta}_w \approx 0 \Rightarrow \ddot{\theta}_e \approx 0\}} M_e = M_c + M_{loss:drv} \\ \Rightarrow M_e &= \frac{M_{w,right} + M_{w,left}}{i_t i_f} + M_{loss:drv} \end{aligned} \quad (4.7)$$

The mean value of the calculated engine torque for each measurement was used as elements in the engine map matrix. The mean value of the throttle position was used to sort the measurement for values in Table 4.2. To get the mean value of the throttle position equal to the table value linear interpolation was used. From measurement done for each RPM and each throttle position an engine map was created, see Figure 4.19 for a 3-D contour plot of a developed engine map.

When measurements for the engine map were performed, the pedal robot was used to get a stable gas pedal position and its position was also logged to create a pedal map. The pedal map uses gas pedal position and engine speed as input and throttle position as output. The measurements were done for fixed throttle positions to create a pedal map where all unique pedal position values were extracted and used as axis values. See Table 4.4 for the pedal position used in the pedal map. The engine speeds used in the pedal map are the same as for the engine map, see Table 4.3. This method was used, instead of performing a separate measurement series with fixed pedal position, to save time and to use the same data to create both maps. See Figure 4.20 for a 3-D contour plot of the developed pedal map.

| | | | | | | |
|-------|-------|-------|-------|-------|-------|---|
| 0 | 0.090 | 0.120 | 0.130 | 0.150 | 0.160 | ↔ |
| 0.200 | 0.250 | 0.255 | 0.290 | 0.330 | 0.360 | ↔ |
| 0.365 | 0.405 | 0.420 | 0.430 | 0.440 | 0.460 | ↔ |
| 0.470 | 0.480 | 0.490 | 0.500 | 0.505 | 0.510 | ↔ |
| 0.515 | 0.520 | 0.525 | 0.530 | 0.535 | 0.540 | ↔ |
| 0.560 | 0.570 | 0.580 | 0.585 | 0.590 | 0.600 | ↔ |
| 0.630 | 0.635 | 0.650 | 0.655 | 0.660 | 0.670 | ↔ |
| 0.690 | 0.700 | 0.710 | 0.720 | 0.730 | 1.000 | |

Table 4.4: Gas pedal position [-] used in the pedal map.

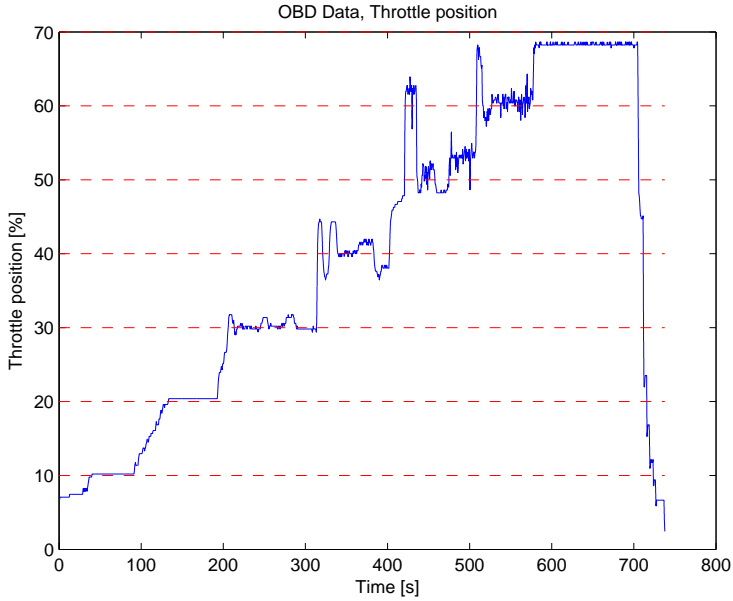


Figure 4.17: Throttle position for a constant speed test for 2500 RPM engine speed and 3rd gear. Measurements have been done for throttle positions 10, 20, ... , 70 % (red dashed lines).

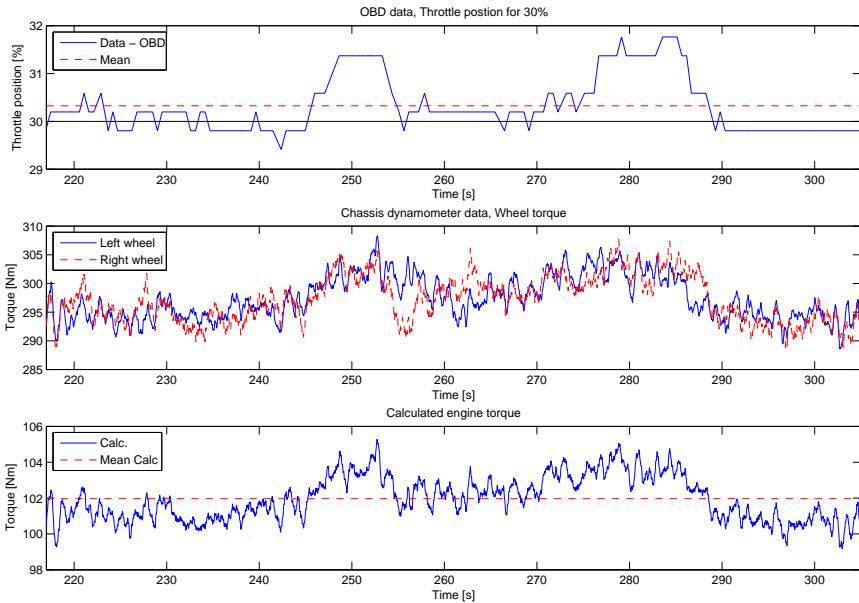


Figure 4.18: Throttle position, wheel torque and engine torques for measurements done for 30 % throttle position for 2500 RPM engine speed and 3rd gear.

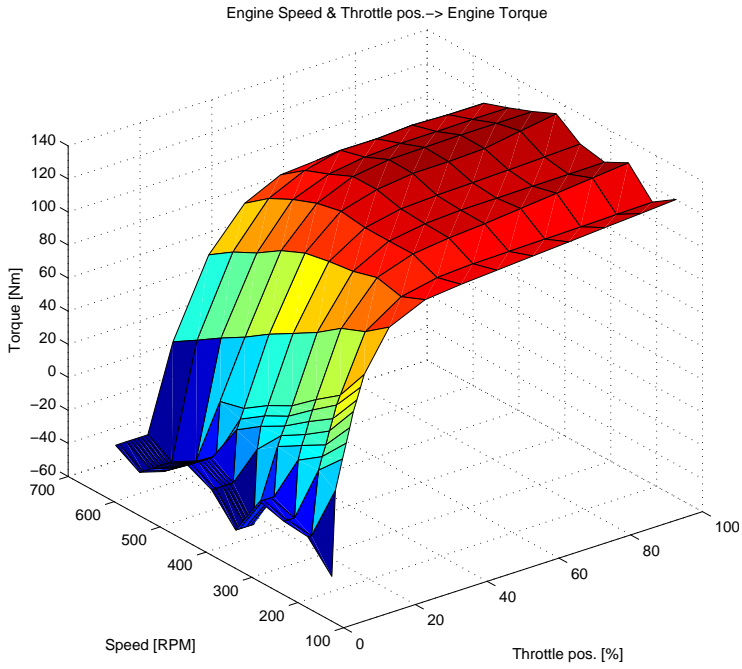


Figure 4.19: 3-D contour plot of the engine map.

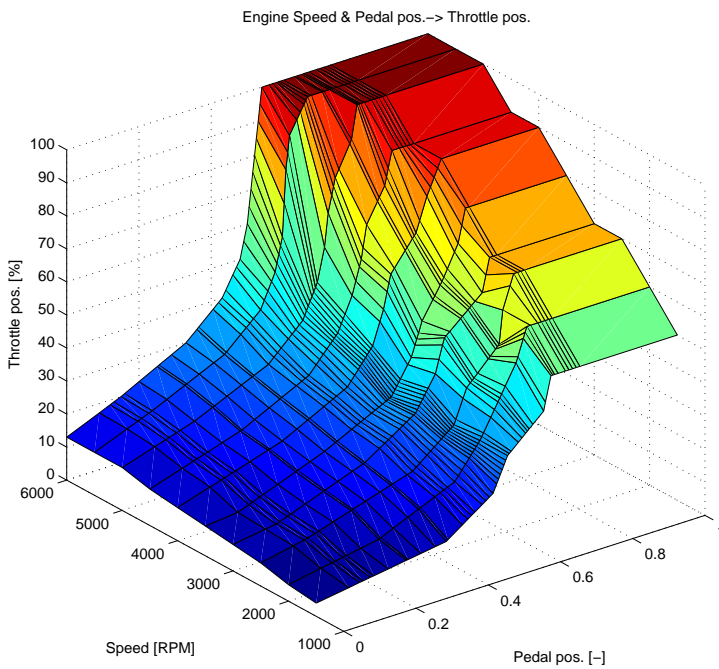


Figure 4.20: 3-D contour plot of the pedal map.

4.5 Engine lag element

The lag elements time constant τ_c in 3.3 was estimated from measurement data where steps in pedal position have been done in a constant speed test. The time constant is the time it takes for the system to reach 63 % of the steady-state value. See Figure 4.21 and Figure 4.22 for examples of step data, the time constants in the examples is 0.209 s and 0.210 s respectively. The time constant used in the powertrain model was the mean time constant of 20 steps in pedal position which was approximately 0.214 s.

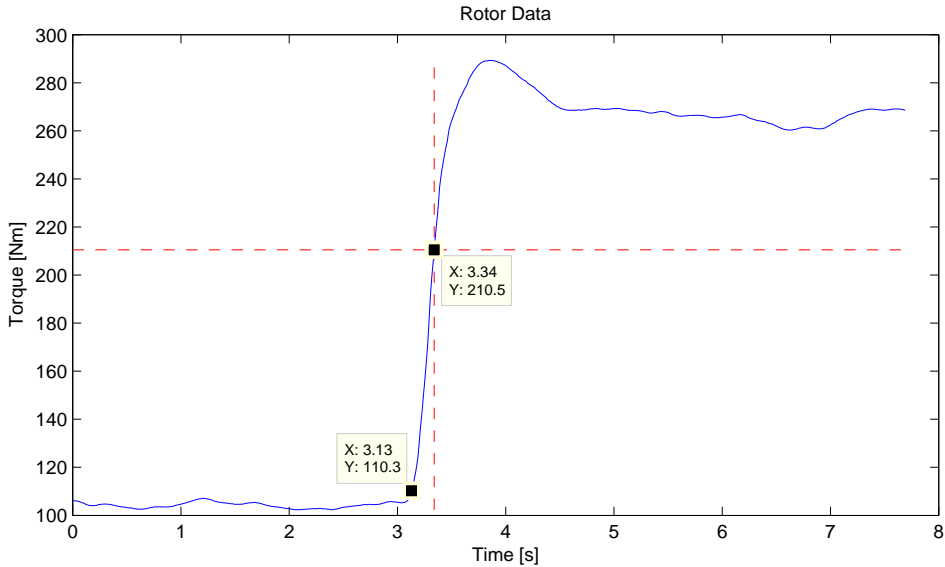


Figure 4.21: Wheel torque from the chassis dynamometer and pedal position from the pedal robot for a constant speed test with step in gas pedal position from 0.2 to 0.4 for 5th gear and 2000 RPM. The point where the red dashed lines intersect is 63 % of the steady-state value.

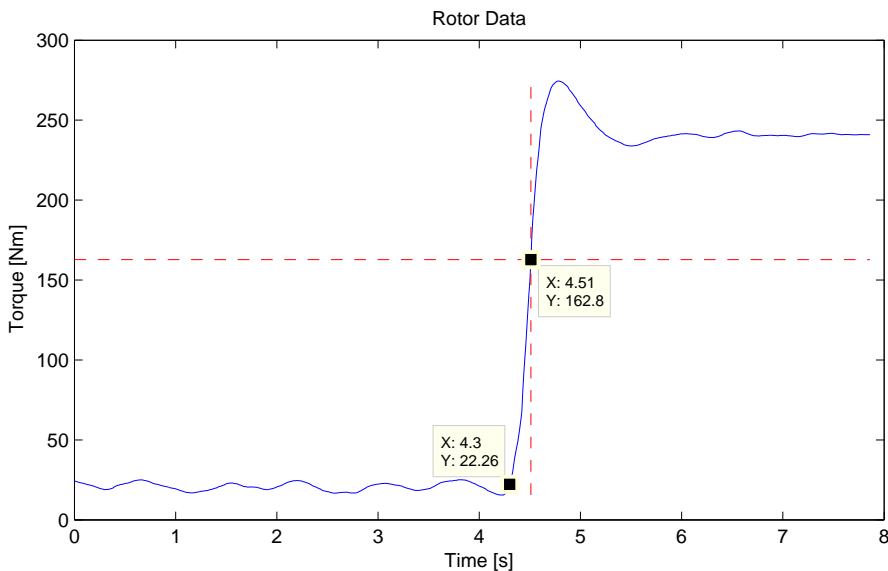


Figure 4.22: Wheel torque from the chassis dynamometer and pedal position from the pedal robot for a constant speed test with step in gas pedal position from 0.1 to 0.3 for 4th gear and 4000 RPM. The point where the red dashed lines intersect is 63 % of the steady-state value.

5

Model validation

This chapter presents validation data for the maps, the standalone powertrain model and the powertrain model integrated into the vehicle model.

5.1 Engine and pedal map validation

The engine and pedal maps were validated with measured data from a constant speed test as inputs and comparing the results from the maps with the measured data. Pedal position and engine speed were used as inputs in the validation and the resulting throttle position and engine torque from the maps were compared with the measured validation data.

Several constant speed tests were performed with various engine speeds and throttle positions to be able to validate different areas of the maps. Measurements were also performed for values between the elements of the map to test the map interpolation.

To be able to get stable measurement values for engine speeds of 1500 RPM and 2500 RPM 3rd gear and higher had to be used. For engine speeds below 1500 RPM the chassis dynamometer can not rotate the wheels for all gears. For 1st gear and all engine speeds the measurements from the chassis dynamometer oscillates. Which is also the case for 2nd gear at engine speed of 1500 RPM, 2250 RPM, 2500 RPM and 2750 RPM. However stable measurements can be obtained for 2nd gear for engine speeds of 2000 RPM, 3000 RPM and higher. Due to the restrictions on the chassis dynamometer the engine and pedal map were created with measurements performed in 3rd and 4th gear.

In Figure 5.1 the pedal position for 20 %, 30 %, 35 % and 60 % throttle position is presented for 2nd, 3rd, 4th and 5th gear for an engine speed of 2000 RPM. In the figure it can be seen that the pedal position for 3rd, 4th and 5th gear were almost the same for all of the presented throttle positions. However the pedal position for 2nd gear was approximately 0.2 higher than the other pedal positions for all of the presented throttle positions. This caused the pedal map to give incorrect values for 2nd gear which can be seen in Figure 5.2. In the figure it can be observed that the engine map is very sensitive at higher throttle positions for example at 120 s there is a small change in throttle position but it gives a large change in the engine torque. However if the measured throttle position was used as input for the engine map it gives a correct engine torque which can be seen in Figure 5.3.

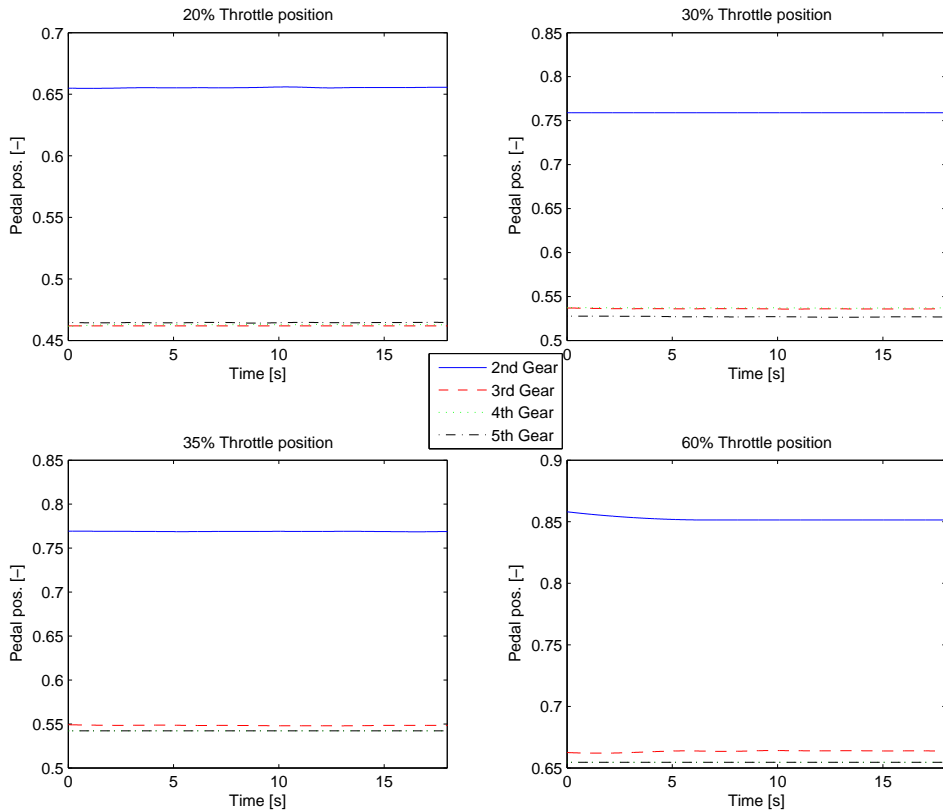


Figure 5.1: Pedal position plots for 20, 30, 35 and 60 % throttle position for an engine speed of 2000 RPM. Each plot shows the necessary pedal position to obtain the given throttle position for 2nd, 3rd, 4th and 5th gear.

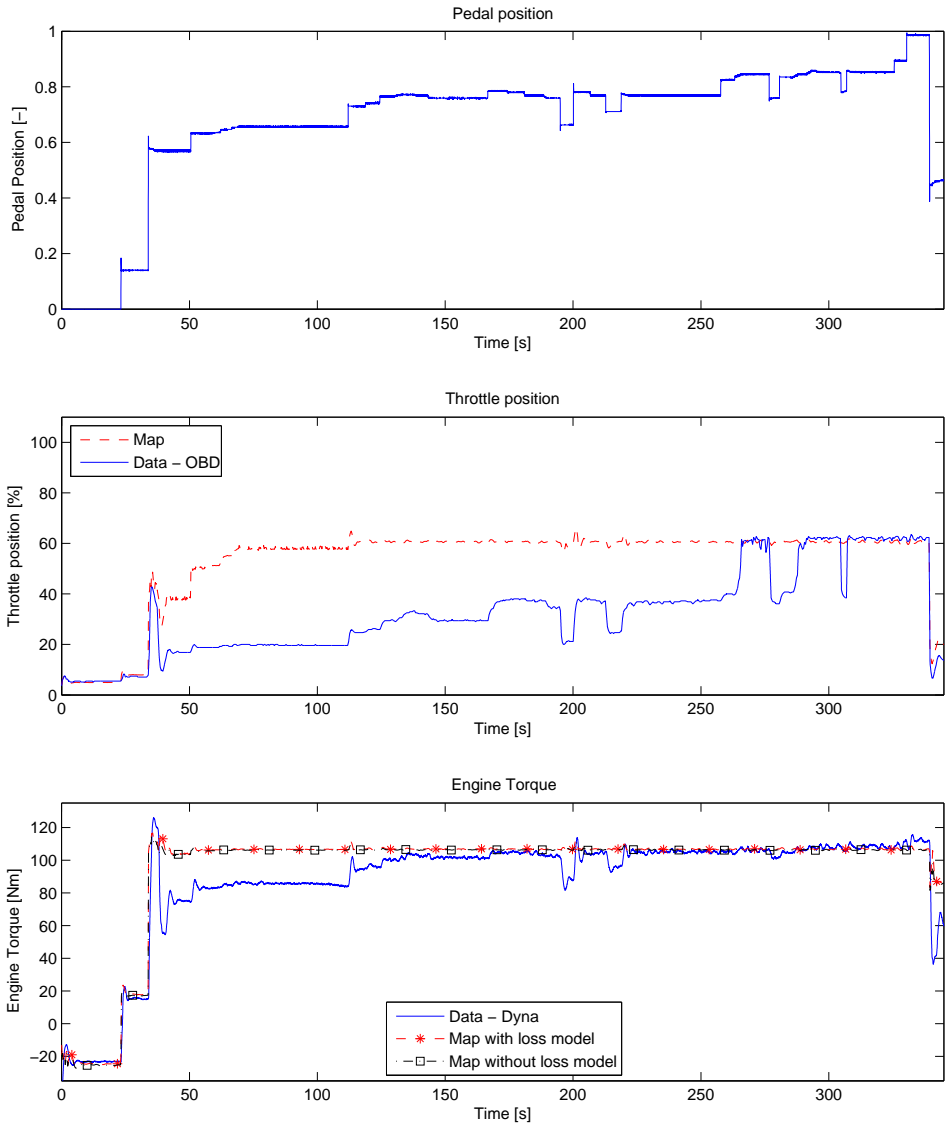


Figure 5.2: Engine and pedal map validation plot for constant speed test with 2000 RPM and 2nd gear. The solid blue line is measured data and the red dashed line is the data from the map with measured pedal position and engine speed as inputs.

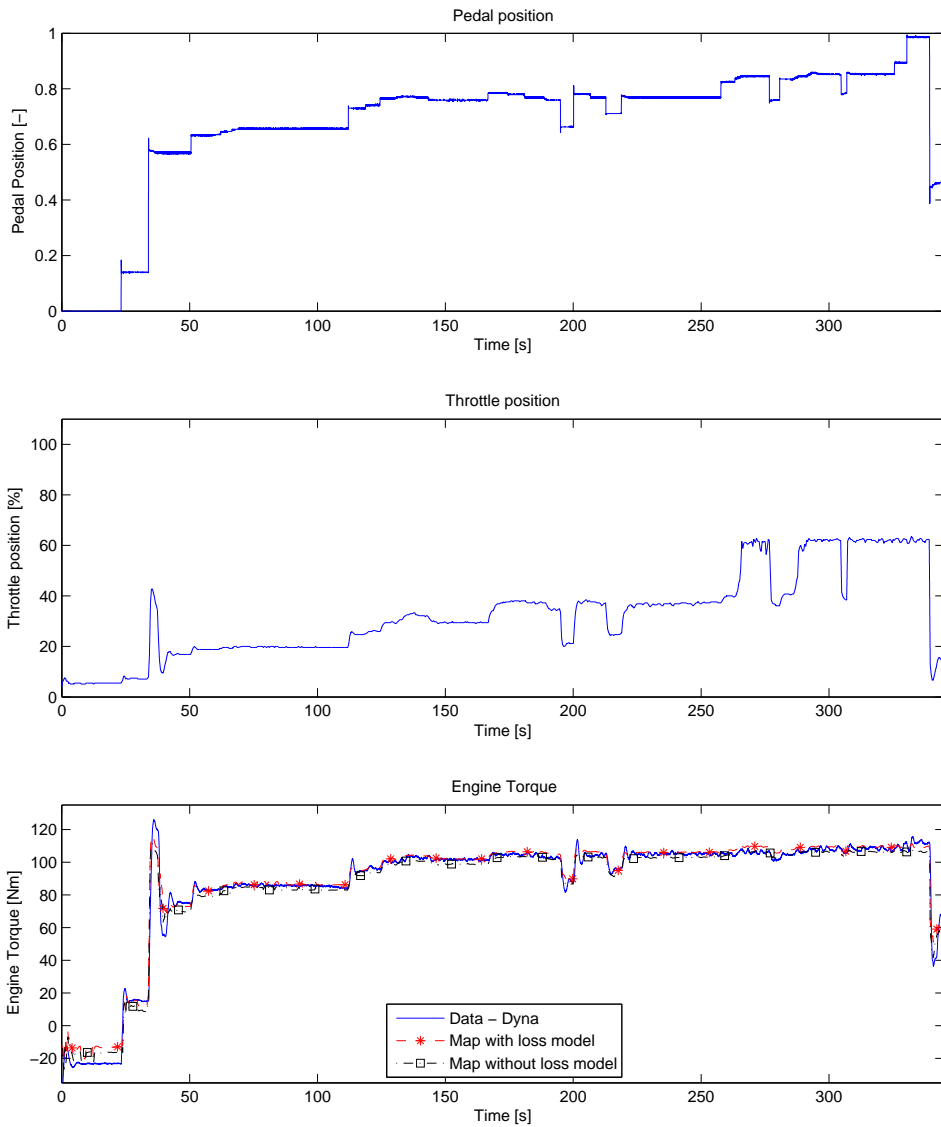


Figure 5.3: Engine map validation plot for constant speed test with a engine speed of 2000 RPM and 2nd gear. The solid blue line is measured data and the red dashed line is the data from the map with measured throttle position and engine speed as inputs.

For higher engine speeds such as 3000 RPM the pedal position for 2nd, 3rd, 4th and 5th gear were almost the same which can be seen in Figure 5.4. The pedal positions were approximately 0.01-0.015 from each other for all of the presented throttle positions. In addition the maps give correct outputs when comparing with measured data which can be seen in Figure 5.5, which presents the results from the maps for an engine speed of 3000 RPM and 2nd gear. The throttle position from the pedal map in Figure 5.5 was a little off for some pedal positions but the resulting engine torque matches well with the measured data. Engine speeds from 3000 RPM and above that uses 2nd gear and higher have similar behaviour as 3000 RPM, see Figure 5.6 and Figure 5.7 for results from the maps for an engine speed of 4000 RPM (4th gear) and 5000 RPM (5th gear) respectively.

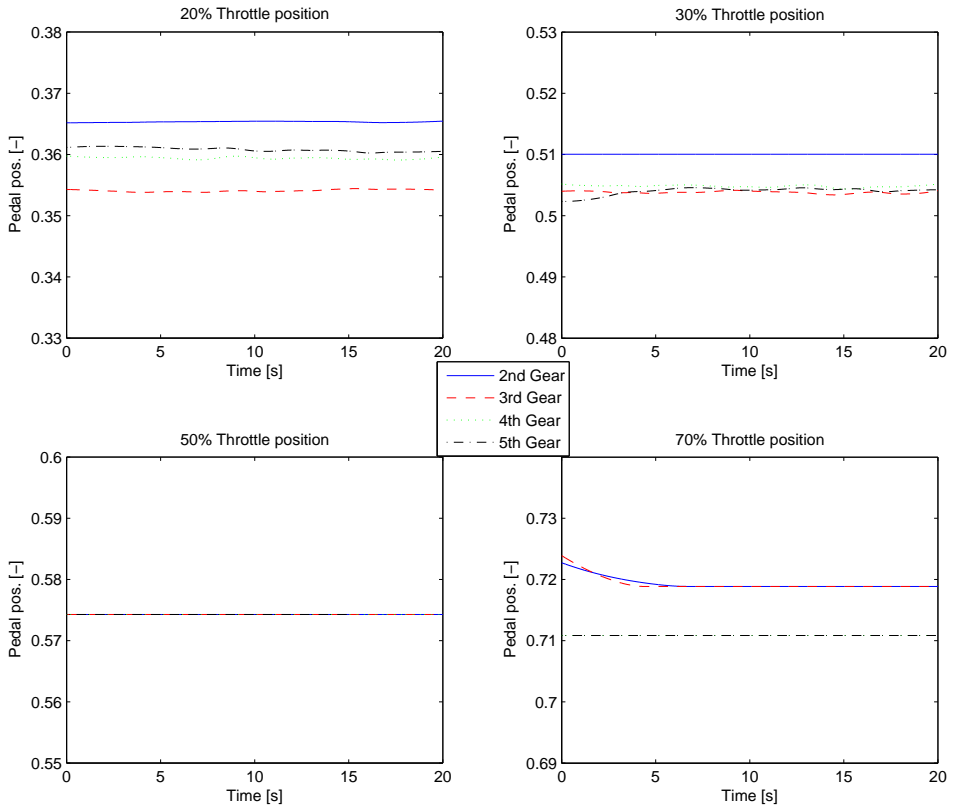


Figure 5.4: Pedal position plots for 20, 30, 50 and 70 % throttle position for an engine speed of 3000 RPM. Each plot shows the necessary pedal position to obtain the given throttle position for 2nd, 3rd, 4th and 5th gear.

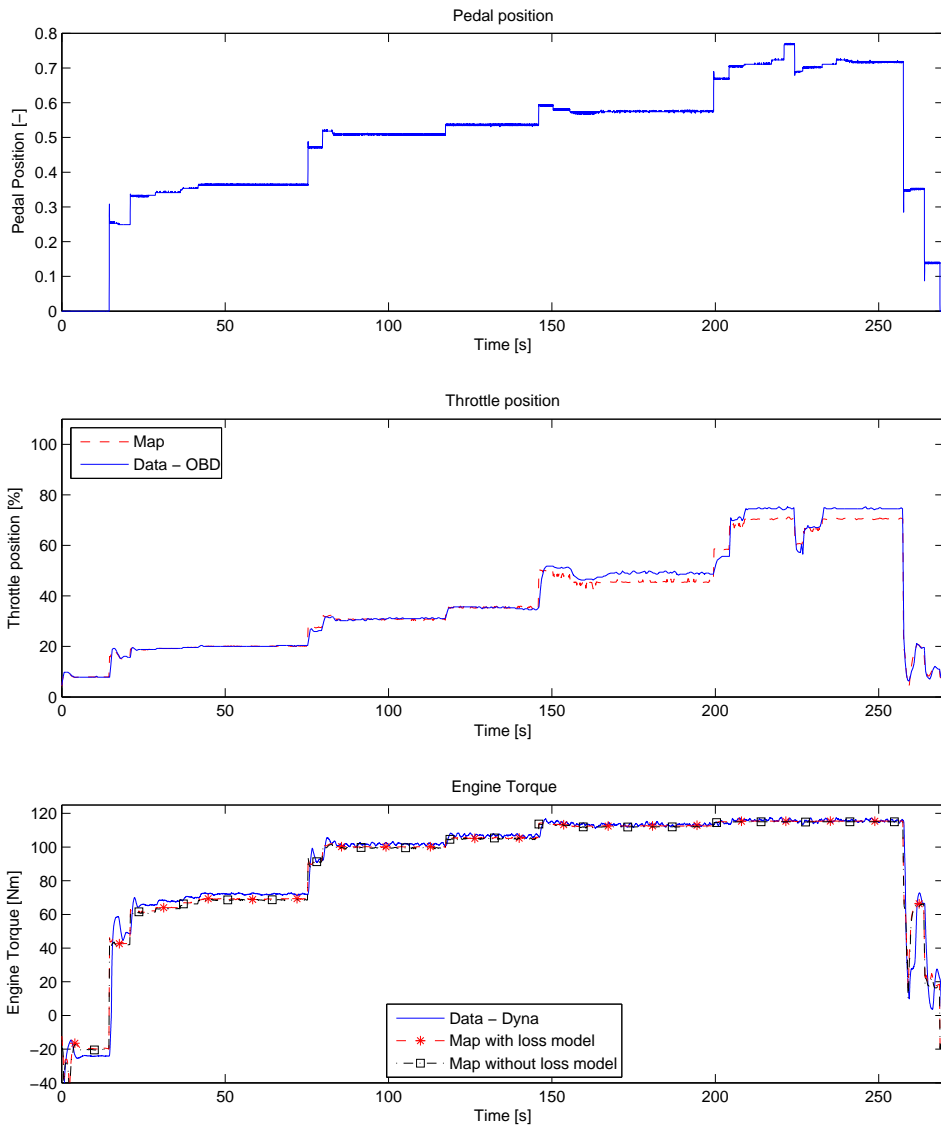


Figure 5.5: Engine and pedal map validation plot for constant speed test with a engine speed of 3000 RPM and 2nd gear. The solid blue line is measured data and the red dashed line is the data from the map with measured pedal position and engine speed as inputs.

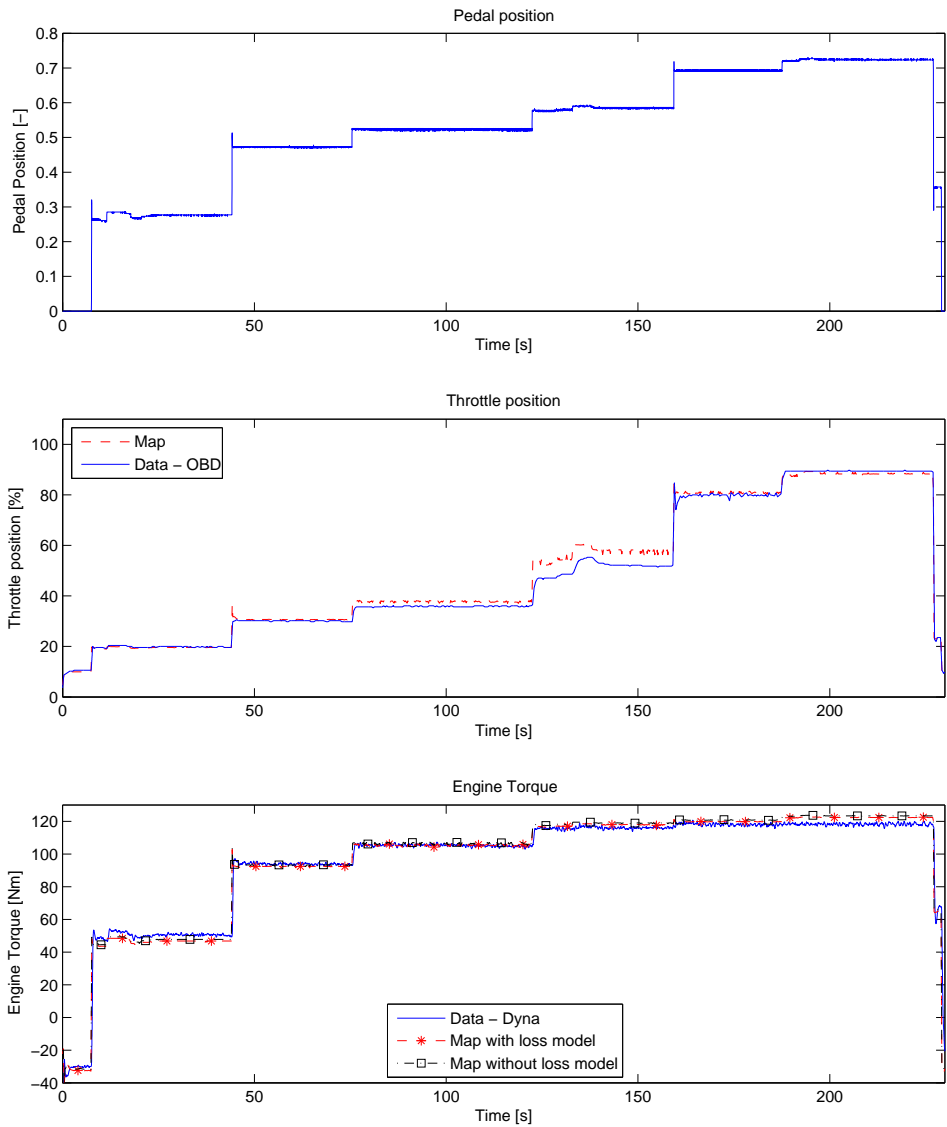


Figure 5.6: Engine and pedal map validation plot for constant speed test with a engine speed of 4000 RPM and 4th gear. The solid blue line is measured data and the red dashed line is the data from the map with measured pedal position and engine speed as inputs.

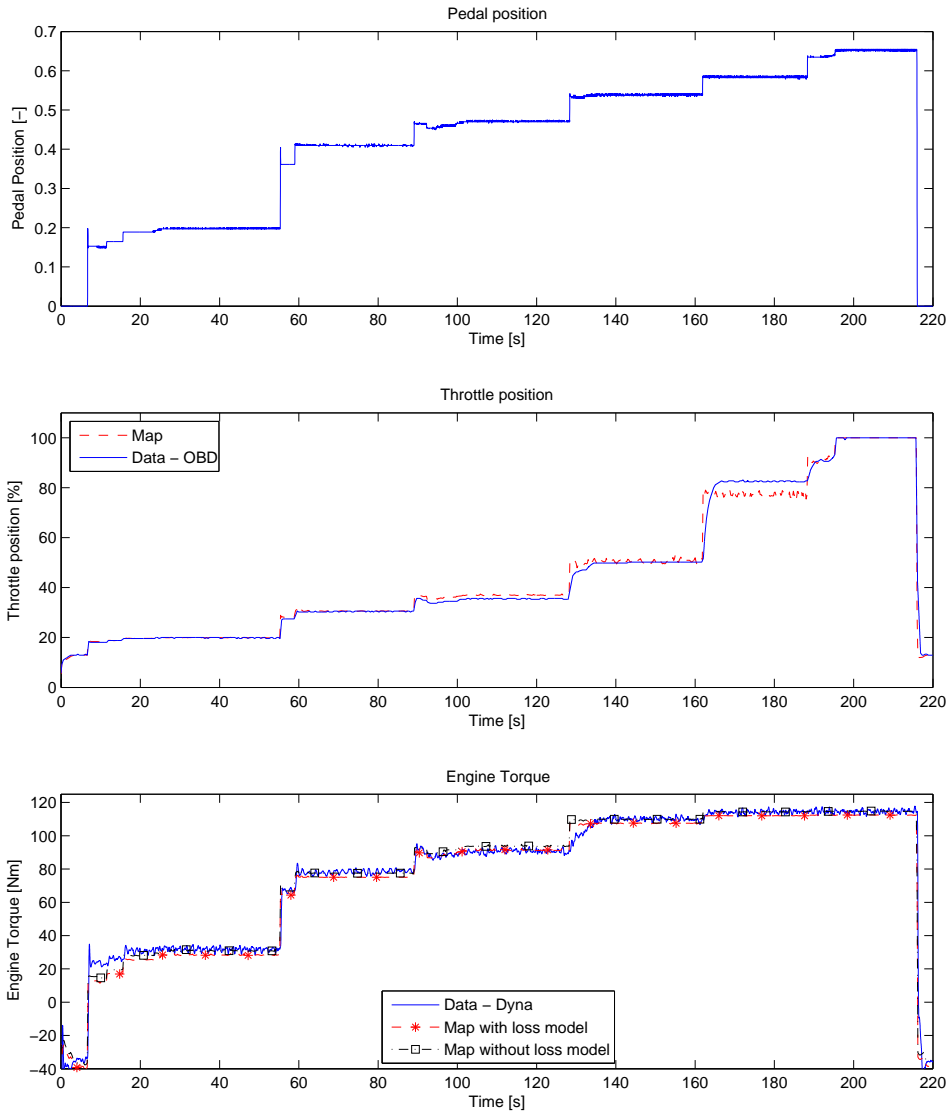


Figure 5.7: Engine and pedal map validation plot for constant speed test with a engine speed of 5000 RPM and 5th gear. The solid blue line is measured data and the red dashed line is the data from the map with measured pedal position and engine speed as inputs.

For values between elements of the maps that are interpolated the maps gave values that were close to the measured data. In Figure 5.8 results from the maps for an engine speed of 2250 RPM and 3rd gear can be seen. The throttle position in the figure is a little off for most pedal position but the engine torque is only $\approx 4 - 5$ Nm off from the measured data.

From Figure 5.1 and Figure 5.4 it can be observed that the same pedal position for each gear do not give the same throttle position for all engine speeds. Because the pedal map was created with measurements performed in 3rd and 4th gear it will give values that do not coincide with the validation data for some areas of the map.

In Figures 5.5 - 5.8 it can be observed that the static error for the engine torque is relatively small and the map data is very close to the validation data. During changes in the engine torque such as at 10 s in Figure 5.5 and at 130 s in Figure 5.7 it can be observed that the map data rises faster than the validation data and there are no overshoot. For the throttle position the static error is larger for higher throttle position but it has a lower impact on the results from the engine map. This is because for higher throttle positions the difference in engine torque between throttle positions is smaller, see Figure 5.7 at 160 s and Figure 5.8 at 160 s. During changes in throttle position the model data rises faster than the validation data and there are no overshoot. Overall the maps gives good results that is similar to the validation data.

Because the throttle position was available from the OBD two maps were created to investigate them separately. From the maps validation in this section it was determined that the pedal map gave incorrect throttle positions for some pedal positions and gears. This in turn caused the engine map to give incorrect engine torque due to it's input being the throttle position from the pedal map, see Figure 5.2. However if the measured throttle positions was used as a input for the engine map its output matched the measured validation data well, see Figure 5.3. By using two maps and investigating them separately it was easier to identify the fault in the pedal map than if a single map was used. With a single map however there would have been no need to extrapolate values to fill empty elements in the map to get a square matrix. Furthermore there would have been no need investigate the idle throttle positions to determine the idle torque for different engine speeds, because for a single map 0 gas pedal position would have covered it.

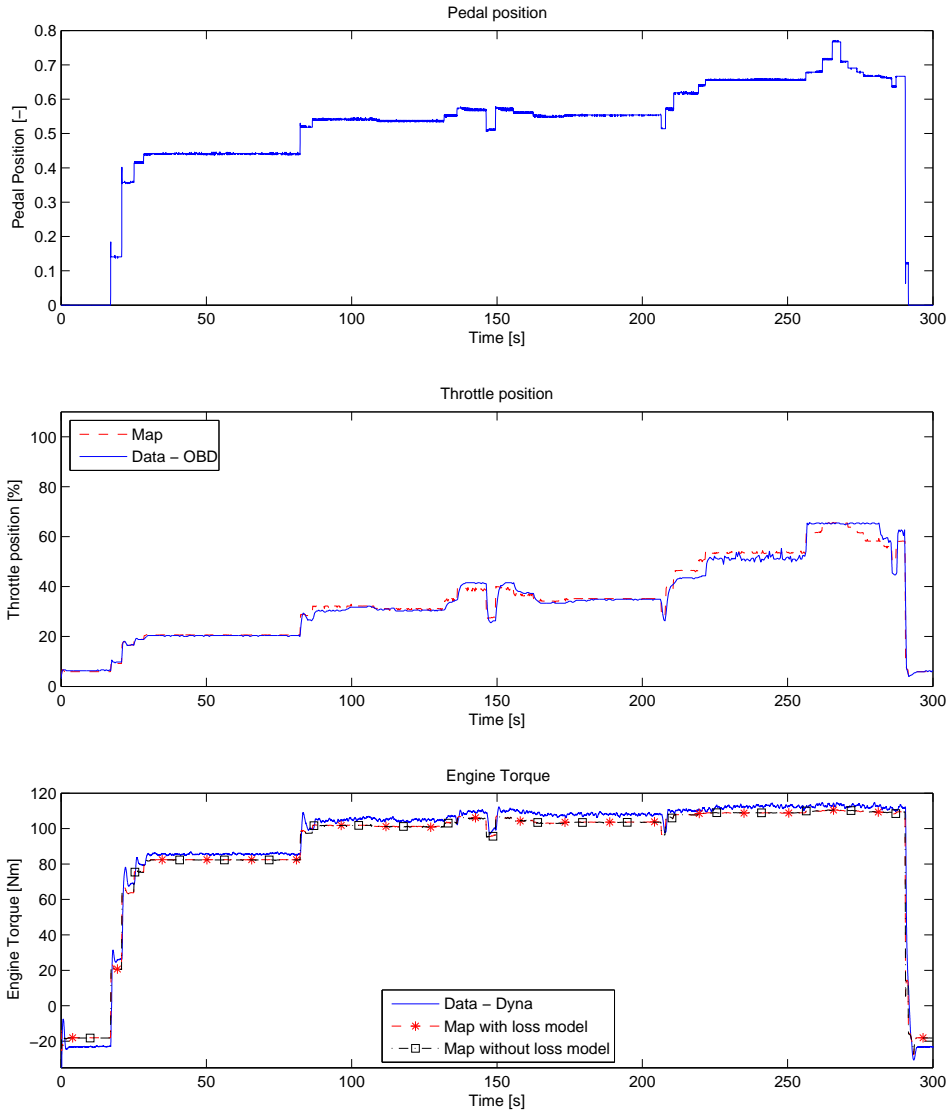


Figure 5.8: Engine and pedal map validation plot for constant speed test with a engine speed of 2250 RPM and 3rd gear. The solid blue line is measured data and the red dashed line is the data from the map with measured pedal position and engine speed as inputs.

The engine torque with and without loss model has been presented in the figures in this section to determine its contribution, see Section 4.3 for details on the loss model. The engine torque in the engine map without loss model was estimated as 4.7 with $M_{loss:drv} = 0$. To determine which gives better results the root mean square error (RMSE) for the engine torques have been calculated where the data from the chassis dynamometer are seen as the true value. The RMSE for the presented figures and some additional cases can be seen in Table 5.1. In the table it can be observed that the map without loss model has lower error for most of the cases which means that it has a better fit. The RMSE for the cases where the engine map row has been created with one gear and validated with a higher gear the error is larger, this is because the driveline losses compensates to much. As the map with loss model gives a larger error overall than the map without loss model it may not be enough to model the driveline losses as a steady state friction torque using a loss map.

| Case | RMSE with | RMSE without | Diff |
|---------------------|-----------|--------------|-----------|
| 1500 RPM & 4th gear | 4.877 Nm | 4.859 Nm | 0.018 Nm |
| 1500 RPM & 5th gear | 6.957 Nm | 7.134 Nm | -0.177 Nm |
| 2000 RPM & 3rd gear | 4.558 Nm | 4.003 Nm | 0.555 Nm |
| 2000 RPM & 4th gear | 6.593 Nm | 4.766 Nm | 1.826 Nm |
| 2000 RPM & 5th gear | 7.731 Nm | 3.936 Nm | 3.795 Nm |
| 2250 RPM & 3rd gear | 4.168 Nm | 4.228 Nm | -0.059 Nm |
| 2250 RPM & 4th gear | 6.327 Nm | 4.993 Nm | 1.334 Nm |
| 2250 RPM & 5th gear | 8.025 Nm | 5.469 Nm | 2.557 Nm |
| 3000 RPM & 2nd gear | 4.201 Nm | 4.405 Nm | -0.204 Nm |
| 3000 RPM & 3rd gear | 6.686 Nm | 6.466 Nm | 0.220 Nm |
| 3000 RPM & 4th gear | 4.917 Nm | 3.783 Nm | 1.134 Nm |
| 3000 RPM & 5th gear | 7.113 Nm | 4.613 Nm | 2.500 Nm |
| 4000 RPM & 3rd gear | 3.294 Nm | 3.013 Nm | 0.280 Nm |
| 4000 RPM & 4th gear | 3.896 Nm | 4.151 Nm | -0.255 Nm |
| 4000 RPM & 5th gear | 4.439 Nm | 4.077 Nm | 0.362 Nm |
| 5000 RPM & 4th gear | 3.906 Nm | 3.500 Nm | 0.406 Nm |
| 5000 RPM & 5th gear | 4.095 Nm | 2.773 Nm | 1.322 Nm |
| 5500 RPM & 4th gear | 8.905 Nm | 8.720 Nm | 0.185 Nm |

Table 5.1: Root mean square error for the engine torque from the map with and without loss model for the cases in the figures in this section. The Diff column is the difference between the RMSE with loss model and RMSE without loss model.

5.2 Standalone powertrain model validation

The developed model was validated with dynamic test data from road resistance tests in the chassis dynamometer for different cases. The measured gas and clutch pedal position and the wheel speeds were used as inputs for the model. For all the testcases the vehicle started parked. The testcases used to validate the model were:

- Case 1:** The vehicle was driven while gear-shifting up sequentially to a designated gear. At the designated gear the driver released the gas pedal and let the engine braking slow the vehicle down. When the engine speed dropped to approximately 1000 RPM the driver engaged the clutch to avoid the engine from stalling.
- Case 2:** The vehicle was driven while gear-shifting up sequentially to a designated gear but one gear was skipped. At the designated gear the driver released the gas pedal and let the engine braking slow the vehicle down. When the engine speed dropped to approximately 1000 RPM the driver engaged the clutch to avoid the engine from stalling.
- Case 3:** The vehicle was driven while gear-shifting up sequentially to a designated gear. At the designated gear the driver started gear-shifting down sequentially back to first gear.

In Figures 5.9 - 5.12 it can be observed that the wheel torque is always incorrect for 1st gear and for some plots the 2nd gear. The wheel torque is incorrect because the pedal map is incorrect for 1st and 2nd gear because it was created from data for 3rd and 4th gear. The wheel torque for 3rd, 4th and 5th gear for the simulated data matches well with the measured data. The results from the comparison of the wheel torques coincide with the results from the map validation in Section 5.1. In addition it can be observed that the engine speed races during gear shift, due to the engine speed being calculated from the engine torque with the help of an integral.

In first gear there are negative spikes in the wheel torque when the vehicle starts from standing still and when gear-shifting down to 1st gear. In Figure 5.9 a negative spike can be seen between 585 s and 590 s. The negative spike was removed by a logic circuit that sets the wheel torque to zero when the model is in 1st gear and the engine torque is negative, see Section 3.1. In Figure 5.10 the same test case as in Figure 5.9 can be observed but the spike is removed.

In Figure 5.10 validation plots for Case 1 going up to 4th gear is presented. During engine braking from 613 s to 627 s in the figure the simulated wheel torque matches the measured wheel torque which means that the model handles engine braking well.

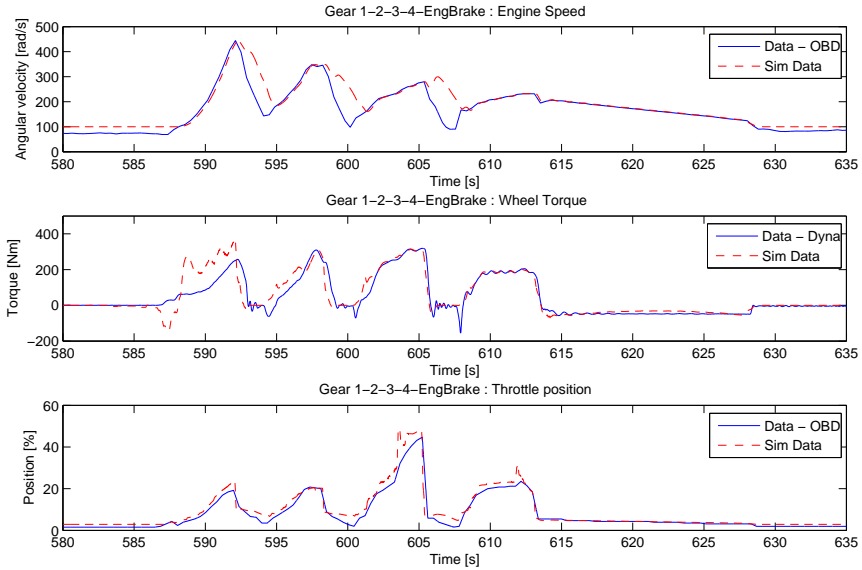


Figure 5.9: Powertrain model, without logic circuit to remove negative spike, validation plots for a road resistance test run with 1st, 2nd, 3rd, 4th gear and then engine braking to a complete stop. The solid blue line is measured data and the red dashed line is the data from the simulated model.

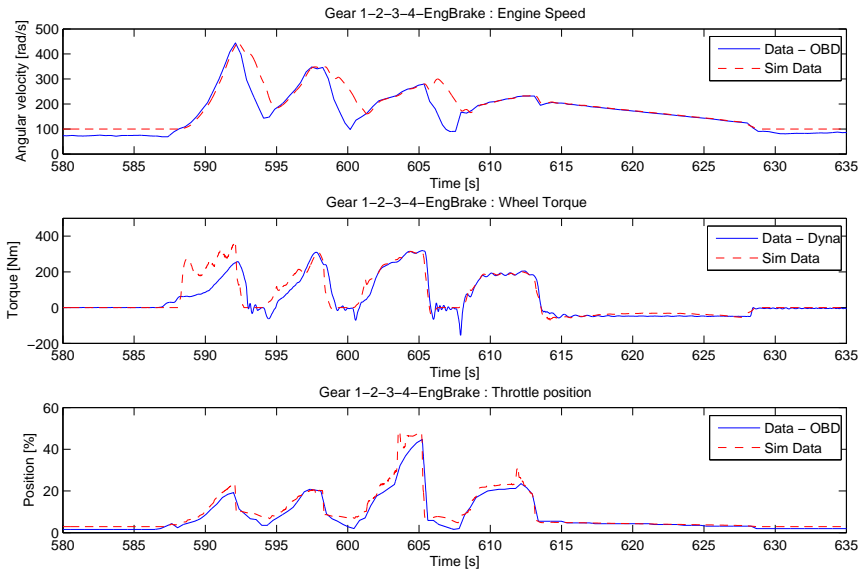


Figure 5.10: Powertrain model validation plots for a road resistance test run with 1st, 2nd, 3rd, 4th gear and then engine braking to a complete stop. The solid blue line is measured data and the red dashed line is the data from the simulated model.

In Figure 5.11 validation plots for Case 2 going up to 4th gear and skipping 3rd gear is presented. In the figure 3rd gear have been skipped but the wheel torque matches well with the measured data. During engine braking from 935 s and 947 s in the figure the wheel torque behaves as in Figure 5.10. That is the simulated wheel torque is close to the to measured wheel torque.

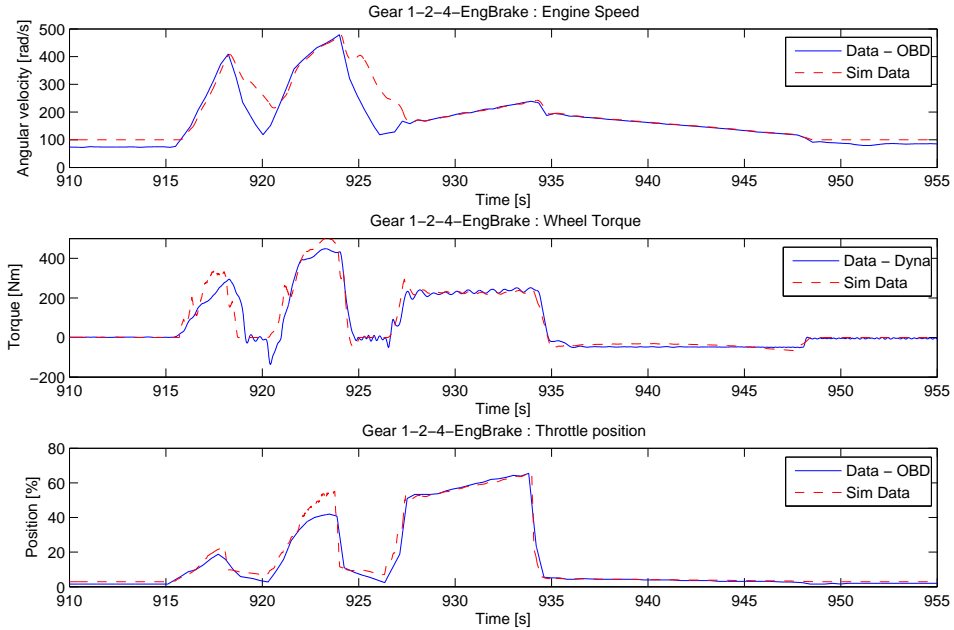


Figure 5.11: Powertrain model validation plots for a road resistance test run with 1st, 2nd, 4th gear and then engine braking to a complete stop, 3rd gear is skipped. The solid blue line is measured data and the red dashed line is the data from the simulated model.

In Figure 5.12 validation plots for Case 3 going up to 5th gear and back down to 1st gear is presented. When gear-shifting down in the figure the wheel torque still matches well with the measured data for gears higher than first gear.

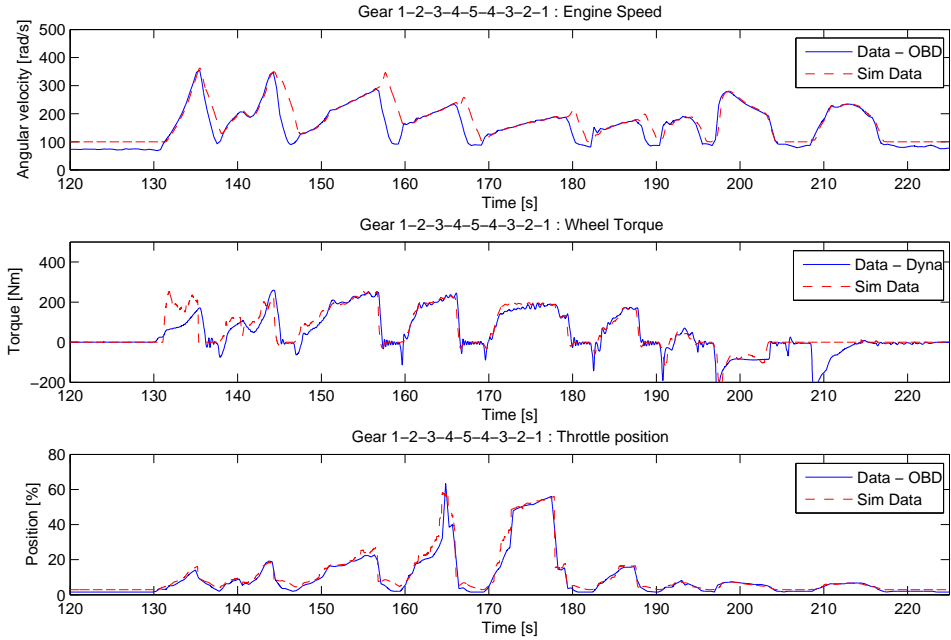


Figure 5.12: Powertrain model validation plots for a road resistance test run with 1st, 2nd, 3rd, 4th and 5th gear then back down with 4th, 3rd, 2nd and 1st gear. The solid blue line is measured data and the red dashed line is the data from the simulated model.

5.3 Integrated powertrain model validation

To validate the developed powertrain model integrated into the vehicle model its behaviour was compared to the existing vehicle model. The validation was focused on the vehicle model behaviour and not comparing the models results because the two vehicle models are for different vehicles and they are modelled differently. The vehicles have different gear ratios, engine size, vehicle parameters etc. The difference was clearly visible if the same gas and clutch pedal positions were used as inputs for both vehicle models, see Figure 5.13. In the figure it can be observed that there is a large difference in the results when the same pedal position is used, which seems to indicate that the models handles the pedal positions differently. However to compare the behaviour the gas pedal position used for the existing vehicle model was scaled down so that both models results were in the same range, see Figures 5.14 - 5.16. The measured gas and clutch pedal positions were used as inputs as in the standalone powertrain model validation. The wheel speed however was not used as input because it was available from the vehicle model.

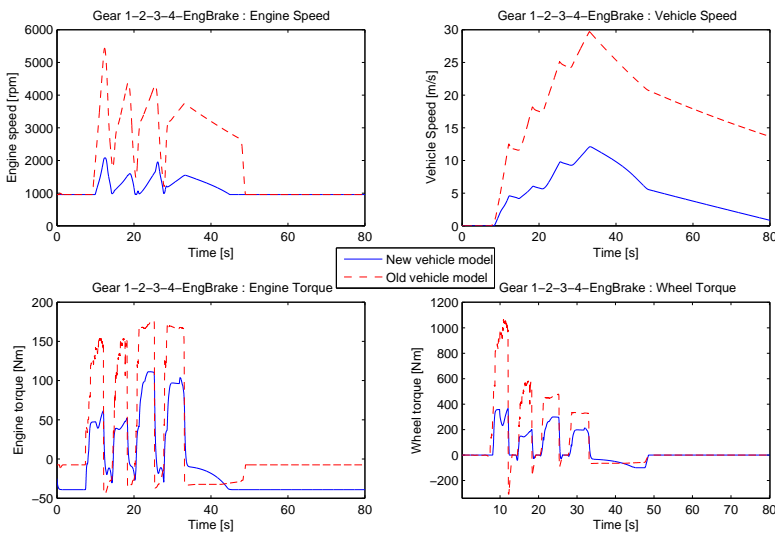


Figure 5.13: Comparison plots of the vehicle models with the same gas and clutch pedal positions. The blue curve is for the developed powertrain model integrated into the vehicle model and the red dashed curve is for the existing vehicle model.

The vehicle model uses several vehicle parameters such as height of center of gravity, moment of inertia for pitch, roll and yaw, wheel base, etc. Some of the models vehicle parameters were changed to coincide with the Golf V however not all of them because some were not available from the Golf V. The parameters for vehicle mass, frontal area of the vehicle, air drag coefficient, rolling resistance coefficient and wheel radius were changed in the vehicle model to the values used in the chassis dynamometer presented in Table 2.2. The mismatch in the vehicle parameters for the Golf V and the ones used in the vehicle model may have an impact on the vehicle model result.

In Figure 5.14 comparison plots of the vehicle models are presented for pedal data from a road resistance test run with 1st, 2nd, 3rd, 4th gear and then engine braking to a complete stop. The pedal data for the existing vehicle model has been scaled down so that the model results are in the same range.

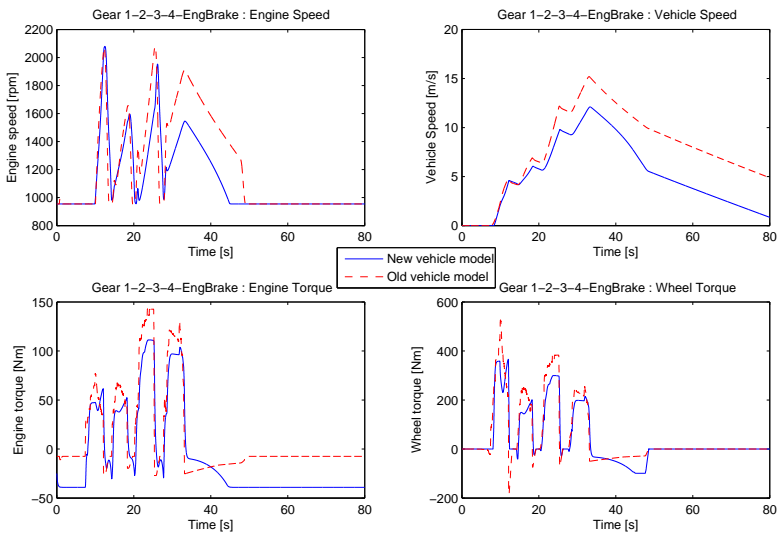


Figure 5.14: Comparison plots of the vehicle models with the scaled down gas pedal position for the existing vehicle model. The pedal positions are from a road resistance test run with 1st, 2nd, 3rd, 4th gear and then engine braking to a complete stop. The blue curve is for the developed powertrain model integrated into the vehicle model and the red dashed curve is for the existing vehicle model.

In Figure 5.15 comparison plots of the vehicle models are presented for pedal data from a road resistance test run with 1st, 2nd, 4th gear and then engine braking to a complete stop, 3rd gear is skipped. The pedal data for the existing vehicle model has been scaled down so that the model results are in the same range. In the figure it can be observed that both vehicle models can handle gear skipping as the engine and wheel torque between 2nd and 4th gear looks normal.

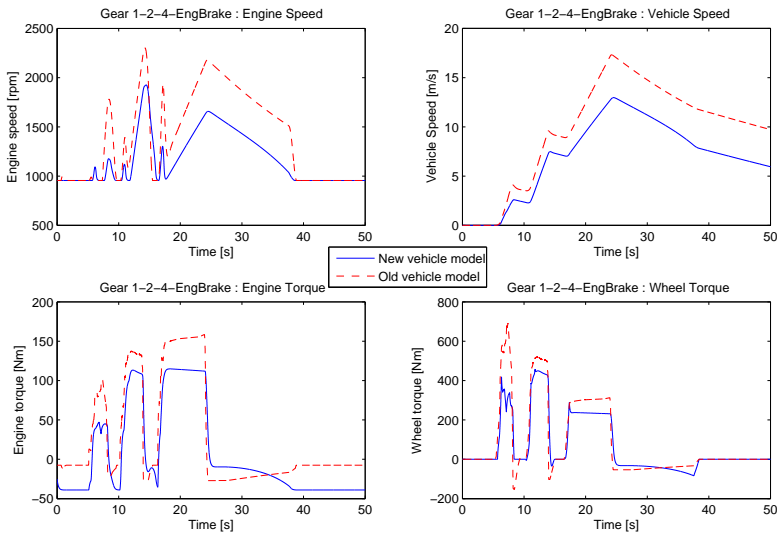


Figure 5.15: Comparison plots of the vehicle models with the scaled down gas pedal position for the existing vehicle model. The pedal positions are from a road resistance test run with 1st, 2nd, 4th gear and then engine braking to a complete stop, 3rd gear is skipped. The blue curve is for the developed powertrain model integrated into the vehicle model and the red dashed curve is for the existing vehicle model.

In Figure 5.16 comparison plots of the vehicle models are presented for pedal data from a road resistance test run with 1st, 2nd, 3rd, 4th and 5th gear then back down with 4th, 3rd, 2nd and 1st gear. The pedal data for the existing vehicle model has been scaled down so that the model results are in the same range. The developed powertrain model uses a logic circuit to remove negative spikes in the wheel torque when the vehicle starts from standing still and when gear-shifting down to 1st gear. The logic circuit sets the wheel torque to zero when the model is in 1st gear and the engine torque is negative. This can be observed in Figure 5.16 between 90 s to 100s. By setting the wheel torque to zero when it is negative the vehicle and engine speed do not decrease as fast as it should. However large negative spikes in the wheel torque is undesirable when the vehicle model is used in the driving simulator.

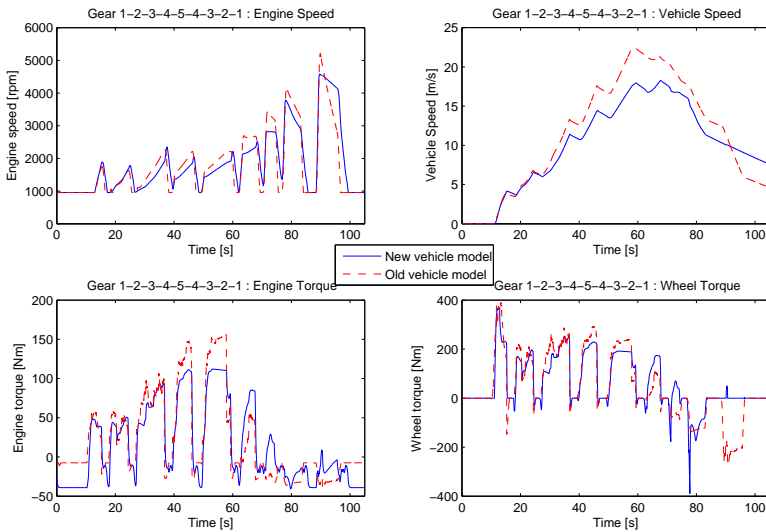


Figure 5.16: Comparison plots of the vehicle models with the scaled down gas pedal position for the existing vehicle model. The pedal positions are from a road resistance test run with 1st, 2nd, 3rd, 4th and 5th gear then back down with 4th, 3rd, 2nd and 1st gear. The blue curve is for the developed powertrain model integrated into the vehicle model and the red dashed curve is for the existing vehicle model.

In Figures 5.14 - 5.16 it can be observed that the engine and wheel torques for the vehicle model with the developed powertrain model is slightly time delayed compared to the existing vehicle model. This is because the developed powertrain model uses a lag element to model the time delay from a change in pedal position to a change in wheel torque, which the existing vehicle model do not. Furthermore the engine and wheel torque for the existing vehicle model is a lot more noisy than for the vehicle model with the developed powertrain model. This is because of the lag element which filters the signal and makes it smoother. The general behaviour of the vehicle models however are similar. The changes in engine and wheel torques, vehicle speeds and engine speeds occur at the correct times and have no excessive spikes. This indicates that the vehicle model with the developed powertrain model has a correct behaviour however the correctness of the vehicle model results needs further investigation. The correctness of the vehicle model with the developed powertrain model can be investigated by comparing the model results with measurement data however this was not carried out due to hardware problems and time restrictions.

6

Conclusion

A powertrain model for a Golf V with a non-turbo combustion engine and manual gearbox have been developed and validated. In addition a methodology to parametrize the model for a vehicle has been presented. The methodology have not been tested on a second vehicle but the data used to parametrize the powertrain model is mostly from the chassis dynamometer and the pedal robot which is available for all vehicles. By using non-invasive sensors the vehicle to model can easily be changed because no extra sensors have to installed in the vehicle.

However some of the tests need engine speed, throttle position, lambda and intake manifold pressure data from the OBD. Most cars and light trucks today have OBD installed but the PIDs available may vary. If the throttle position is not available from the vehicle a single map from pedal position to engine torque can be used instead of the current two maps. The single map will however still have the problem of the pedal map discussed in Section 5.1. The intake manifold pressure from the OBD have been used to estimate the engine losses but was not used in the model. The air/fuel ratio (lambda) was used to check if any fuel was injected in the engine during the measurements for the inertia estimations. The inertia estimations can be performed without lambda measurements however without the measurements the results may be incorrect due to the engine producing torque. Only the engine speed is necessary from the OBD to be able to perform the tests.

The validation of the maps showed that they gave good results for engine speeds from 3000 RPM and above that uses 2nd gear and higher, as shown in Section 5.1. For engine speeds below 3000 RPM the maps gave good results for 3rd gear and higher but for gears lower than 3rd the maps gave values that did not match up with the validation data. Which was because the maps were created using measurements performed in 3rd and 4th gear and the pedal position for each gear do not give the same throttle position for all engine speeds. For example at an engine speed of 2000 RPM the same pedal position for 2nd gear and 3rd gear gives different throttle positions.

The validation of the standalone powertrain model matched the results for the maps because it gave good data fit for measurements performed in 3rd gear and higher, as shown in Section 5.2. For measurements performed in 1st gear and most of 2nd gear the standalone powertrain model generally gave to high values for the engine torque but the engine speed and throttle position gave good results. The higher engine torque for lower gears is due to the pedal map giving incorrect values. During the standalone powertrain model validation several driving cases were tested such as engine braking, gear-shifting and skipping gears. The standalone powertrain model performed well for all of the presented driving cases.

To validate the developed powertrain model integrated into the vehicle model its behaviour was compared to the existing vehicle model, as shown in Section 5.3. The developed powertrain model integrated into the vehicle model has a correct behaviour however the correctness of the vehicle model results need further investigation by comparing the model results with measurement data. This was however not carried out due to hardware problems and time restrictions.

6.1 Future Work

This section lists some possible improvements to the powertrain model.

Improve pedal and engine map at lower gears

The engine and pedal maps can be improved by extending the pedal map to a 3 dimensional map with the gear as a third input. With gear as a input the map can have different pedal positions for each gear which fixes the problem that the same pedal position for different gears gives different throttle positions.

As it is currently not possible to obtain good measurements for 1st and 2nd gear for all engine speeds due to restrictions on the chassis dynamometer. For example at engine speeds of 1500 RPM and 2500 RPM for 2nd gear the measurement oscillates. If it becomes possible to obtain good measurements for lower gears the map could also be improved by complementing it with the measurements.

Turbocharged engine model

The developed powertrain model is for non-turbocharged combustion engine. To be able to model a larger selection of vehicles the engine model can be extended to handle turbocharged combustion engines.

Vehicle parameters

Most of the vehicle parameters used in the vehicle model were kept as the existing values because they were not available from the Golf V. By investigating the vehicle parameters of the Golf V and changing to the correct parameters in the vehicle model may have an impact on the vehicle model result.

Investigate vehicle model results

The correctness of the results from the vehicle model with the developed powertrain can be investigated by comparing the model results with measurement data from the chassis dynamometer.

Bibliography

- [1] Anders Andersson, Peter Nyberg, Håkan Sehnammar, and Per Öberg. Vehicle powertrain test bench co-simulation with a moving base simulator using a pedal robot. SAE International Journal of Passenger Cars - Electronic and Electrical Systems, 6(1):169–179, May 2013. Cited on page 2.
- [2] Auto-data. Wiki automotive catalog. URL <http://www.auto-data.net/en/>. Cited on page 38.
- [3] Marius Bataus, Andrei Maciac, Mircea Oprean, and Nicolae Vasiliu. Automotive clutch models for real time simulation. Proceedings of the Romanian Academy, Series A, 12(2):109–116, 2011. Cited on page 4.
- [4] A Crowther, N Zhang, D K Liu, and J K Jeyakumaran. Analysis and simulation of clutch engagement judder and stick-slip in automotive powertrain systems. Proceedings of the Institution of Mechanical Engineers, Part D: Journal of Automobile Engineering 2004, 218:1427–1446, December 2004. Cited on page 4.
- [5] Pietro Dolcini, Carlos Canudas de Wit, and Hubert Béchart. Improved optimal control of dry clutch engagement. Proceedings of the 16th IFAC World Congress, 2005. Cited on page 4.
- [6] Lars Eriksson and Ingemar Andersson. An analytic model for cylinder pressure in a four stroke SI engine. SAE Transactions, Journal of Engines, 2002-01-0371, 111(3), September 2003. Cited on page 3.
- [7] Lars Eriksson and Lars Nielsen. Modeling and Control of Engines and Drivelines. John Wiley & Sons, 2014. Cited on pages 4, 5, 17, 23, and 38.
- [8] Outils OBD Facile. Obd modes and pids. URL <http://www.outilsobdfacile.com/obd-mode-pid.php>. Cited on page 13.
- [9] Peter Van den Bossche Joeri Van Mierlo and Gaston Maggetto. Models of energy sources for ev and hev: fuel cells, batteries, ultracapacitors, flywheels and engine-generators. Journal of Power Sources 128, page 76–89, 2004. Cited on page 1.

- [10] Robert Johansson. Modeling of engine and driveline related disturbances on the wheel speed in passenger cars. Master's thesis, Linköping University, SE-581 83 Linköping, 2012. Cited on pages 2 and 3.
- [11] Adam Lagerberg. Control and Estimation of Automotive Powertrains with Backlash. PhD thesis, Chalmers Univeristy of Technology, 2004. Cited on page 5.
- [12] Andreas Myklebust and Lars Eriksson. Torque model with fast and slow temperature dynamics of a slipping dry clutch. In 8th IEEE Vehicle power and propulsion conference, Seoul, South Korea, 2012. Cited on page 4.
- [13] Andreas Myklebust and Lars Eriksson. Road slope analysis and filtering for driveline shuffle simulation. In E-COSM'12 – IFAC Workshop on Engine and Powertrain Control, Simulation and Modeling, Paris, France, October 2012. Cited on page 4.
- [14] Andreas Myklebust and Lars Eriksson. The effect of thermal expansion in a dry clutch on launch control. In AAC'13 – 7th IFAC Symposium on Advances in Automotive Control, Tokyo, Japan, 2013. Cited on page 4.
- [15] Mohit Hashemzadeh Nayeri. Cylinder-by-cylinder torque model of an si-engine for real-time applications. Master's thesis, Linköping University, SE-581 83 Linköping, 2005. Cited on page 3.
- [16] Tomas Nilsson. Optimal engine operation in a multi-mode CVT wheel loader. Technical report, 2012. LiU-TEK-LIC-2012:32, Thesis No. 1547. Cited on page 3.
- [17] Tomas Nilsson, Anders Fröberg, and Jan Åslund. Optimal operation of a turbocharged diesel engine during transients. SAE International Journal of Engines, SAE Paper: 2012-01-0711, 5(2):571–578, May 2012. Cited on page 3.
- [18] Magnus Nordenborg. Model based driveline control. Master's thesis, Linköpings Universitet, SE-581 83 Linköping, 2005. Cited on pages 2 and 5.
- [19] Per Öberg, Peter Nyberg, and Lars Nielsen. A new chassis dynamometer laboratory for vehicle research. SAE International Journal of Passenger Cars - Electronic and Electrical Systems, 6(1):152–161, May 2013. Cited on pages 10 and 12.
- [20] Magnus Pettersson. Driveline Modeling and Control. PhD thesis, Linköpings Universitet, May 1997. Cited on pages 2 and 4.
- [21] G. Rizzoni, L. Guzzella, and B.M. Baumann. Unified modeling of hybrid electric vehicle drivetrains. IEEE/ASME Transactions on Mechatronics, 4: 246–257, 1999. Cited on page 3.
- [22] Ramteen Sioshansi and Paul Denholm. Emissions impacts and benefits of plug-in hybrid electric vehicles and vehicle to grid services. Environ. Sci. Technol., page 1199–1204, 2009. Cited on page 1.

-
- [23] Shan-Chi Tsai and M. R. Goyal. Dynamic turbocharged diesel engine model for control analysis and design. SAE Technical Paper 860455, Mars 1986. Cited on pages 2, 3, 17, 18, and 19.



Upphovsrätt

Detta dokument hålls tillgängligt på Internet — eller dess framtida ersättare — under 25 år från publiceringsdatum under förutsättning att inga extraordinära omständigheter uppstår.

Tillgång till dokumentet innebär tillstånd för var och en att läsa, ladda ner, skriva ut enstaka kopior för enskilt bruk och att använda det oförändrat för icke-kommersiell forskning och för undervisning. Överföring av upphovsrätten vid en senare tidpunkt kan inte upphäva detta tillstånd. All annan användning av dokumentet kräver upphovsmannens medgivande. För att garantera äktheten, säkerheten och tillgängligheten finns det lösningar av teknisk och administrativ art.

Upphovsmannens ideella rätt innefattar rätt att bli nämnd som upphovsman i den omfattning som god sed kräver vid användning av dokumentet på ovan beskrivna sätt samt skydd mot att dokumentet ändras eller presenteras i sådan form eller i sådant sammanhang som är kränkande för upphovsmannens litterära eller konstnärliga anseende eller egenart.

För ytterligare information om Linköping University Electronic Press se förlagets hemsida <http://www.ep.liu.se/>

Copyright

The publishers will keep this document online on the Internet — or its possible replacement — for a period of 25 years from the date of publication barring exceptional circumstances.

The online availability of the document implies a permanent permission for anyone to read, to download, to print out single copies for his/her own use and to use it unchanged for any non-commercial research and educational purpose. Subsequent transfers of copyright cannot revoke this permission. All other uses of the document are conditional on the consent of the copyright owner. The publisher has taken technical and administrative measures to assure authenticity, security and accessibility.

According to intellectual property law the author has the right to be mentioned when his/her work is accessed as described above and to be protected against infringement.

For additional information about the Linköping University Electronic Press and its procedures for publication and for assurance of document integrity, please refer to its www home page: <http://www.ep.liu.se/>